



**HAL**  
open science

## The histone chaperones ASF1 and HIRA are required for telomere length and 45S rDNA copy number homeostasis

Adéla Machelová, Martina Nešpor Dadejová, Michal Franek, Lauriane Simon, Samuel Le Goff, Céline Duc, Jasmin Bassler, Martin Demko, Jana Schwarzerová, Sophie Desset, et al.

### ► To cite this version:

Adéla Machelová, Martina Nešpor Dadejová, Michal Franek, Lauriane Simon, Samuel Le Goff, et al.. The histone chaperones ASF1 and HIRA are required for telomere length and 45S rDNA copy number homeostasis. *The Plant Journal*, In press, 10.1111/tpj.17041 . hal-04745954

**HAL Id: hal-04745954**



**<https://hal.science/hal-04745954v1>**

Submitted on 21 Oct 2024

**HAL** is a multi-disciplinary open access archive for the deposit and dissemination of scientific research documents, whether they are published or not. The documents may come from teaching and research institutions in France or abroad, or from public or private research centers.

L'archive ouverte pluridisciplinaire **HAL**, est destinée au dépôt et à la diffusion de documents scientifiques de niveau recherche, publiés ou non, émanant des établissements d'enseignement et de recherche français ou étrangers, des laboratoires publics ou privés.

# The histone chaperones ASF1 and HIRA are required for telomere length and 45S rDNA copy number homeostasis

Adéla Machelová<sup>1,2</sup>, Martina Nešpor Dadejová<sup>1</sup>, Michal Franek<sup>1</sup>, Guillaume Mougeot<sup>3,†</sup>, Lauriane Simon<sup>3</sup>, Samuel Le Goff<sup>3</sup>, Céline Duc<sup>4</sup>, Jasmin Bassler<sup>5</sup>, Martin Demko<sup>6</sup>, Jana Schwarzerová<sup>7,8</sup>, Sophie Desset<sup>3</sup>, Aline V. Probst<sup>3,\*</sup>  and Martina Dvořáčková<sup>1,2,\*</sup> 

<sup>1</sup>Mendel Centre for Plant Genomics and Proteomics, CEITEC, Masaryk University, Brno CZ-62500, Czech Republic,

<sup>2</sup>Laboratory of Functional Genomics and Proteomics, NCBR, Faculty of Science, Masaryk University, Brno CZ-61137, Czech Republic,

<sup>3</sup>iGReD, Université Clermont Auvergne, CNRS, INSERM, BP 38, Clermont-Ferrand 63001, France,

<sup>4</sup>Nantes Université, CNRS, US2B UMR 6286, Nantes F-44000, France,

<sup>5</sup>Gregor Mendel Institute of Molecular Plant Biology, Austrian Academy of Sciences, Vienna Biocenter (VBC), Vienna 1030, Austria,

<sup>6</sup>Core Facility Bioinformatics, CEITEC, Masaryk University, Brno CZ-62500, Czech Republic,

<sup>7</sup>Department of Biomedical Engineering, Faculty of Electrical Engineering and Communication, Brno University of Technology, Brno 616 00, Czech Republic,

<sup>8</sup>Molecular Systems Biology (MOSYS), Department of Functional and Evolutionary Ecology, Faculty of Life Sciences, University of Vienna, Vienna 1030, Austria

Received 19 March 2024; revised 3 September 2024; accepted 6 September 2024.

\*For correspondence (e-mail [martina.dvorackova@ceitec.muni.cz](mailto:martina.dvorackova@ceitec.muni.cz) and [aline.probst@uca.fr](mailto:aline.probst@uca.fr)).

†Present address: Department of Ecoscience, Aarhus University, Aarhus, Denmark

## SUMMARY

Genome stability is significantly influenced by the precise coordination of chromatin complexes that facilitate the loading and eviction of histones from chromatin during replication, transcription, and DNA repair processes. In this study, we investigate the role of the Arabidopsis H3 histone chaperones ANTI-SILENCING FUNCTION 1 (ASF1) and HISTONE REGULATOR A (HIRA) in the maintenance of telomeres and 45S rDNA loci, genomic sites that are particularly susceptible to changes in the chromatin structure. We find that both ASF1 and HIRA are essential for telomere length regulation, as telomeres are significantly shorter in *asf1a1b* and *hira* mutants. However, these shorter telomeres remain localized around the nucleolus and exhibit a comparable relative H3 occupancy to the wild type. In addition to regulating telomere length, ASF1 and HIRA contribute to silencing 45S rRNA genes and affect their copy number. Besides, ASF1 supports global heterochromatin maintenance. Our findings also indicate that ASF1 transiently binds to the TELOMERE REPEAT BINDING 1 protein and the N terminus of telomerase *in vivo*, suggesting a physical link between the ASF1 histone chaperone and the telomere maintenance machinery.

**Keywords:** chromatin, telomeres, histone chaperones, ASF1, HIRA, 45S rDNA, *Arabidopsis thaliana*.

## INTRODUCTION

Chromatin is composed of chains of nucleosomes, each comprising approximately 146 base pairs of DNA wrapped around an octamer of H3, H4, H2A, and H2B histones. Histones exist in the form of different histone variants providing distinct structural and functional attributes to the nucleosome and are subject to numerous post-translational modifications, thereby modifying DNA accessibility and contributing to controlling access of DNA repair, replication, and transcription machinery (Buschbeck & Hake, 2017; Probst et al., 2020). The

accurate storage, deposition, and turnover of histones are mediated by protein complexes called histone chaperones (Li et al., 2019; Typas, 2023).

In yeast, plants, and vertebrates, H3–H4 histones are handled by several histone chaperones, including ANTI-SILENCING FUNCTION 1 (ASF1A and ASF1B) (Le et al., 1997; Moshkin et al., 2002; Zhu et al., 2011), the HISTONE REGULATOR A (HIRA) (Duc et al., 2015; Lamour et al., 1995; Nie et al., 2014; Ray-Gallet et al., 2002), and the CHROMATIN ASSEMBLY FACTOR 1 (CAF-1) complex (Kaufman et al., 1995; Tyler et al., 1999). In *Arabidopsis*

*thaliana*, the latter consists of FASCIATA 1 (FAS1), FASCIATA 2 (FAS2), and MULTICOPY SUPPRESSOR OF IRA 1 (MSI1) (Kaya et al., 2001; Kirik et al., 2006). CAF-1 is responsible for the deposition of H3.1 in a DNA-synthesis-dependent manner (Benoit et al., 2019; Jiang & Berger, 2017; Verreault et al., 1996). The HIRA complex comprising UBINUCLEIN (UBN1 and 2), CABIN 1, and HIRA (Duc et al., 2015; Nie et al., 2014) mainly deposits H3.3 throughout the cell cycle through DNA-synthesis-independent assembly during transcription and DNA repair (Adam et al., 2013; Bouvier et al., 2021; Ray-Gallet et al., 2002; Torne et al., 2020). ASF1 proteins bind H3–H4 dimers without distinguishing between replicative H3.1 and replacement H3.3 histone variants (English et al., 2006; Le Goff et al., 2020).

Despite the strong conservation of histone chaperones and their functions, variations across different model systems provide interesting insight into functional specifications. For instance, yeast has one ASF1 protein, whereas mammals have two paralogs, ASF1A and ASF1B (Abascal et al., 2013). Both interact with CAF-1's middle-size (p60) subunit and are essential for S-phase progression, but only ASF1A interacts with HIRA (Abascal et al., 2013; Groth et al., 2007; Tagami et al., 2004; Tyler et al., 1999). Arabidopsis has also two mostly functionally redundant ASF1 paralogs, with abnormal phenotypes only observed upon the loss of both (Min et al., 2019; Zhu et al., 2011).

Plant ASF1 proteins play a role in replication and DNA repair processes, as evidenced by the altered S phase and sensitivity to replication fork stalling (Zhu et al., 2011), which may relate to its function in buffering excess histones as in mammals (Groth et al., 2007). A recent study showed the formation of HIRA-ASF1A or ASF1B complexes, indicating ASF1's predominant role in replication-independent nucleosome assembly (Zhong et al., 2022).

Arabidopsis plants deficient in ASF1, CAF-1, or HIRA exhibit altered distribution of H3.1 and H3.3 (Kolarova et al., 2021; Otero et al., 2016; Wollmann et al., 2012; Zhong et al., 2022) and changed nucleosome positioning (Duc et al., 2015; Munoz-Viana et al., 2017; Zhong et al., 2022). Notably, *hira* mutants display nucleosome occupancy changes in transcribed regions and heterochromatin (Duc et al., 2015; Nie et al., 2014), while in *fas2* mutants, non-transcribed regions are more affected (Munoz-Viana et al., 2017; Zhong et al., 2022). The nucleosome landscape in *asf1a1b* resembles that of *hira* mutants (Zhong et al., 2022).

Proper chromatin assembly through the accurate deposition, turnover, and modifications of histones is important not only for the stability of the epigenome but also for genome integrity. This is illustrated by the progressive loss of *45S ribosomal RNA* gene copies (*45S rDNA*) or telomeres in *fas1* and *fas2* plants (Mozgova et al., 2010). Due to their

repetitive nature, these loci are challenging to replicate and are especially sensitive to changes in chromatin composition (Dvorackova et al., 2015; Wu et al., 2021).

Telomeres are key elements in resolving the end-replication problem and end protection (McClinck, 1930; Olovnikov, 1992; Richards & Ausubel, 1988). This is mediated through the Shelterin protein complex (de Lange, 2005; Weinert, 2005) and by telomerase (Fajkus et al., 1998; Greider & Blackburn, 1985, 1996). TELOMERE REPEAT BINDING FACTORS 1–3 (AtTRB1–3) are part of Arabidopsis' telomere protective complex (Hofr et al., 2009; Schrupfova et al., 2014, 2019). They interact with components of telomerase (Lermontova et al., 2007; Schorova et al., 2019; Schrupfova et al., 2014), localize to telomeres, and accumulate in the nucleolus (Dreissig et al., 2017; Dvorackova et al., 2010), possibly affecting telomerase function and trafficking, similar to their role in mammals (Lee et al., 2014; Schrupfova et al., 2019; Yang et al., 2002). Additionally, plant telomeres belong to the nucleolus-associated domains (Pontvianne et al., 2013).

Recent work confirmed an old hypothesis that telomere chromatin is arranged in a columnar structure, which may cause higher susceptibility to DNA damage (Fajkus & Trifonov, 2001; Soman et al., 2022). Given that telomeres are enriched in H3.3 (Vaquero-Sedas & Vega-Palas, 2013; Wong et al., 2009), we investigate the roles of H3.3 histone chaperones ASF1 and HIRA in telomere maintenance. We show that they are both necessary to control telomere length and that the two paralogs ASF1A and ASF1B play redundant roles. The function of ASF1 and HIRA in genome stability is not restricted to telomeres, as silent *45S rRNA* gene copies are reactivated and *45S rDNA* copy number is affected in both mutants. Moreover, global heterochromatin organization is reduced in *asf1a1b* mutant plants. Finally, our results from bimolecular fluorescence complementation assays show that ASF1 interacts transiently with the N-terminal domain of telomerase and TRB1 *in vivo*, establishing a link between ASF1 and telomere length control. This highlights the importance of the histone chaperone network in preserving genome stability.

## RESULTS

### ASF1 function is required for telomere length homeostasis

To understand the potential involvement of the histone chaperone ASF1 in telomere maintenance, we first investigated whether the loss of ASF1A and ASF1B in *A. thaliana* affects the homeostasis of telomere repeats, similar to observations in other model species (Jiang et al., 2011; O'Sullivan et al., 2014). To this end, we carried out terminal restriction fragment (TRF) analysis to quantify telomere length in *asf1a1b* double mutants (Figure 1a; Figure S1a). In this assay, genomic DNA is digested by restriction endonucleases, leaving the telomeric DNA intact. From the

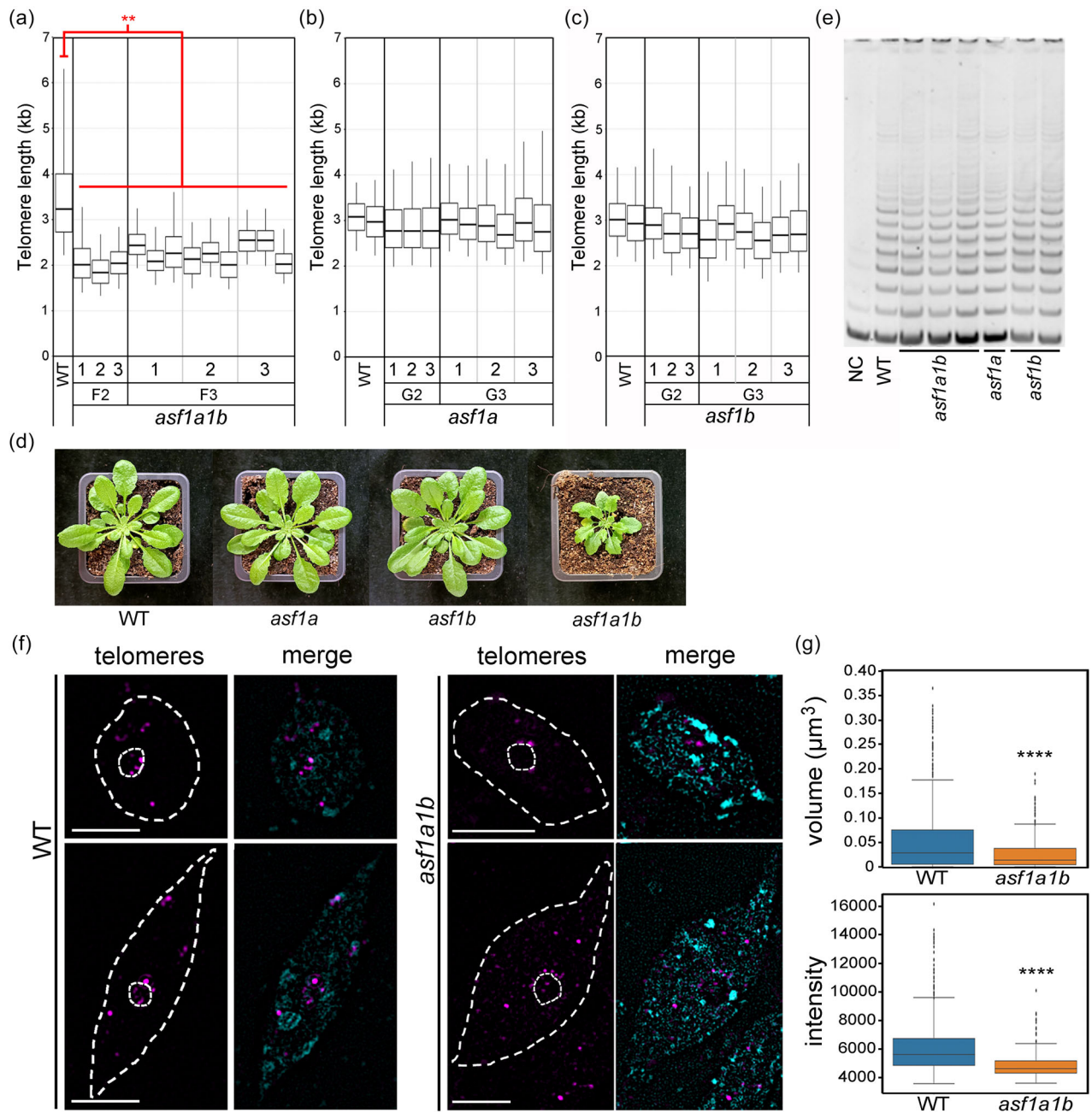


**Figure 1.** Telomeres in *asf1a1b* mutants are shortened without disruption of telomerase activity. (a–c) Telomere length of WT and mutant plants determined by terminal restriction fragment (TRF) analysis with subsequent evaluation of the range of telomere signals by the WALTER software. From the initial generation (F<sub>x</sub>, G<sub>x</sub>) (Zhu et al., 2011), we propagated mutant plants for an additional two generations. (a) *asf1a1b* (F<sub>2</sub> and F<sub>3</sub> generations), (b) *asf1a*, and (c) *asf1b* (G<sub>2</sub> and G<sub>3</sub> generations). Three sister plants (1–3) and their progeny are shown. Box charts present the first and third quartiles separated by the median value. The maximum and minimum telomere lengths are represented by the whiskers above and under the boxes. \*\**P* < 0.05 for *asf1a1b* compared to WT based on *t*-test. For *asf1a* and *asf1b*, the *t*-test showed no significant changes in telomere length compared to WT. (d) Phenotype of *asf1a*, *asf1b*, and *asf1a1b* plants. Representative images of 6-week-old plants. (e) Telomere repeat amplification protocol (TRAP) in WT, *asf1a1b*, *asf1a*, and *asf1b* mutants showed similar telomerase activity in all tested samples. Samples were compared to the protein extract-free reaction buffer used as negative control (NC). (f) Telomere localization pattern obtained by fluorescence *in situ* hybridization (FISH) with consequent super-resolution microscopy (3D SIM) on nuclei of 10-day-old seedlings in WT and *asf1a1b*. Nuclei were probed by the biotin-labeled telomeric probe (magenta), and DNA was counterstained with 4,6-diamidino-2-phenylindole (DAPI, blue). Dashed lines indicate the contours of the nuclei and nucleoli. The scale bar represents 5 μm. (g) Quantification of the mean volume and the intensity of individual telomeric signals in WT and *asf1a1b*; the number of nuclei *N* = 68 in WT and 52 in *asf1a1b*; 3D SIM images. Box charts show the first and third quartiles separated by the median value. The maximum and minimum values are represented by the whiskers above and under the boxes. \*\*\*\**P* < 0.005 based on the Kruskal–Wallis test. Most measured nuclei were of elongated shape, as seen in the bottom image of (f).

initial generation (F<sub>x</sub>), which had been used in a previous study (Zhu et al., 2011), we propagated *asf1a1b* double-mutant plants for an additional two generations (F<sub>2</sub> and F<sub>3</sub>). Compared to wild-type (WT) plants, which have a mean telomere length of around 3 kb, we measured a significantly shorter telomere length of 2 kb in both later generations of *asf1a1b* double mutants. As progressive shortening, for example, in telomerase-deficient plants, can drop beyond this level (Fitzgerald et al., 1999), the observed telomere length of 2 kb may represent a limit specific to *asf1a1b* double-mutant plants. Our results, therefore, show that, compared to mammals, where telomere lengthening is observed upon siRNA suppression of ASF1 homologs (O'Sullivan et al., 2014), the simultaneous loss of plant ASF1A and ASF1B had the opposite effect on telomere maintenance. This suggests functional diversification between plant and mammalian ASF1 proteins in telomere length regulation.

We next asked whether reduced telomere length requires disruption of both *ASF1* genes or if one of the two paralogs plays a major role in telomere length maintenance. Quantification of telomere length in single *asf1a* and *asf1b* mutants showed telomere length comparable to WT (Figure 1b,c; Figure S1b,c). We conclude that the two ASF1 proteins compensate for each other's function in telomere length maintenance. This is consistent with previous work (Zhu et al., 2011) and our observations (Figure 1d) that single mutants do not display macroscopic phenotypic defects. Functional redundancy between ASF1A and ASF1B was also observed in *caf-1* mutant background, as telomere length in *fas1 asf1a*, *fas1 asf1b*, *fas2 asf1a*, and *fas2 asf1b* seedlings is shortened to around 2 kb similar to the telomere size observed in plants deficient for only *FAS1* and *FAS2* as previously shown (Mozgova et al., 2010) (Figure S2a,b). To gain a deeper understanding of the telomere shortening phenotype in *asf1a1b* mutants, we next tested whether telomere shortening could be caused by telomerase malfunction in the double-mutant background. We subjected protein telomerase-enriched extracts from WT and *asf1a1b* mutant plants to the telomere repeat amplification protocol (TRAP) (Kim et al., 1994). Using this assay, we observed an identical level of telomere primer amplification in all examined plants (Figure 1e), indicating that the loss of ASF1 proteins does not affect telomerase function. Given the observed telomere shortening, we next wanted to determine the extent to which the nuclear distribution of telomeres is affected by the loss of ASF1 function. We therefore carried out fluorescence *in situ* hybridization (FISH) for telomere repeats and imaged nuclei using 3D structured illumination microscopy (SIM, Figure 1f). In WT plants, we detected the expected distribution of telomeres with the majority surrounding the nucleolus (Armstrong et al., 2001; Probst et al., 2003). This organization was unaffected in *asf1a1b*

mutants, and the average number of telomere signals was similar (WT = 7.6, *asf1a1b* = 7.3). Detailed quantification revealed a reduction in both the volume and intensity of telomere signals in *asf1a1b* mutants (Figure 1g), consistent with the decrease in telomere length revealed by TRF analysis (Figure 1a).

#### Loss of ASF1 affects 45S rDNA copy number and heterochromatin organization

The reduced telomere length in *asf1a1b* mutant plants recalls observations in the *fas1* and *fas2* mutants, in which occurs also a dramatic 45S rDNA loss (Mozgova et al., 2010). Therefore, we decided to investigate the organization of 45S rDNA by FISH, asking whether ASF1 function is additionally required for maintenance of these repeats. The condensed 45S rDNA signals co-localize with chromocenters as expected and remain compact in *asf1a1b*, with no sign of decondensation (Figure 2a). Since the 45S rDNA signals were significantly smaller in *asf1a1b* (Figure 2a,b), we determined 45S rDNA copy number by quantitative PCR in single WT and *asf1a1b* plants in two different generations (a = F<sub>2</sub> and b = F<sub>4</sub>) (Figure 2c). We consistently found a lower 45S rDNA copy number in *asf1a1b* (Figure 2c), but less pronounced compared to *caf-1* mutants that show strong progressive 45S rDNA loss (30–50% of repeats per generation) (Mozgova et al., 2010; Muchova et al., 2015). To explore whether loss of ASF1 would also impact rRNA gene expression, we analyzed the relative abundance of 45S rDNA variants in rRNA transcripts in the same *asf1a1b* plants. *VAR1* rRNA genes, situated on NOR2 and transcriptionally silent in WT plants (Chandrasekhara et al., 2016; Pontvianne et al., 2013), are expressed in *asf1a1b* mutants, indicating a connection between reduced copy number and transcriptional activation (Figure 2d).

Telomeres and 45S rDNA repeats are important elements of chromosomal architecture, which determines the distribution of genetic material during cell divisions in mitosis and meiosis. Especially changes in telomere functions can cause chromosome instability, for example, by generating chromosome fusions (Jaske et al., 2013; Riha et al., 2001). Therefore, we counted the occurrence of chromosome end-to-end fusions visible as anaphase bridges (Figure S3a,b). This marker of genome instability was not increased in *asf1a1b* when compared to WT, indicating that ASF1 deficiency does not induce chromosome aberrations.

Given that both telomere and 45S rDNA copy numbers are affected, we asked whether ASF1 is required for global maintenance of heterochromatin organization in Arabidopsis. To answer this question, we determined nuclear morphology and chromocenter volume in guard (GC) and pavement cell (PC) nuclei of the cotyledon epidermis (Figure 2e; Figure S3c) using *biom3D*, *bioRxiv*

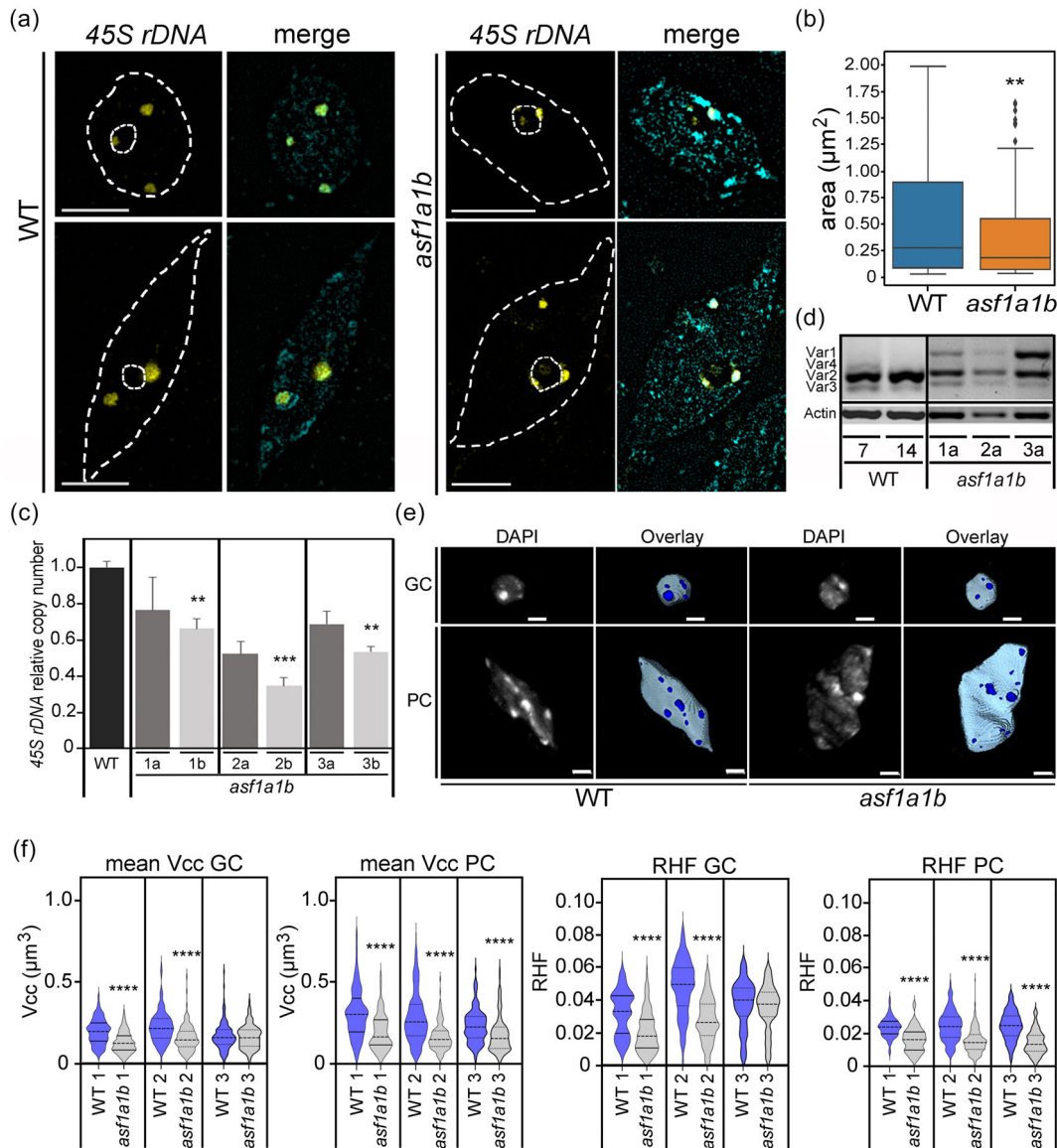


**Figure 2.** Loss of ASF1 causes reduced *45S rRNA* gene copy number and reduced chromocenter volume.

(a) *45S rDNA* localization pattern obtained by fluorescence *in situ* hybridization (FISH) with consequent super-resolution microscopy (2D SIM) on nuclei of 10-day-old WT and *asf1a1b* seedlings. *45S rDNA* probe (yellow) and DNA counterstained with 4,6-diamidino-2-phenylindole (DAPI, blue); dashed lines indicate contours of nuclei and nucleoli. The scale bar represents 5  $\mu\text{m}$ .

(b) Quantification of the area of *45S rDNA* signals in WT and *asf1a1b*; number of nuclei  $N = 161$  in WT and 106 in *asf1a1b*; 2D-SIM images. Box charts show the first and third quartiles separated by the median value. The maximum and minimum values are represented by the whiskers above and under the boxes.  $**P < 0.05$ ; compared to WT, Kruskal–Wallis test. Most measured nuclei were of elongated shape, as seen in the bottom image of (a).

(c) *45S rDNA* copy number was determined by quantitative PCR (qPCR) in 4-week-old leaves in WT and three different *asf1a1b* biological replicates (F2 and F4 generations). Sister plants (1a–3a; F2) and their progeny (1b–3b; F4; mean of two biological replicates). Relative *45S rDNA* copy number, with WT set to 1 and using *UBIQUITIN 10* as a reference, is shown.  $***P < 0.01$ ,  $**P < 0.05$  compared to WT, two-sided *t*-test.

(d) Reverse transcription followed by PCR (RT-PCR) amplification of *45S rRNA* variant transcripts in 14-day-old seedlings in three sister plants of *asf1a1b* mutants compared to 7-day-old and 14-day-old seedlings of WT. *ACTIN* was used as a control.

(e) Representative guard cell (GC) and pavement cell (PC) nuclei from cotyledon epidermis of WT and *asf1a1b* seedlings. Left: DAPI-stained nuclei. Right: Overlay of segmented nucleus (light blue) and chromocenters (dark blue) on top of the DAPI-stained nucleus. Scale bars represent 2  $\mu\text{m}$ .

(f) Quantification of mean chromocenter volume (Vcc) and relative heterochromatin fraction (RHF) in GC and PC of three independent biological replicates (10-day-old (WT and *asf1a1b* 1 and 2) or 14-day-old (WT and *asf1a1b* 3) seedlings). GC: WT 1,  $n = 193$ ; WT 2,  $n = 189$ ; WT 3,  $n = 154$ ; *asf1a1b* 1,  $n = 147$ ; *asf1a1b* 2,  $n = 194$ ; *asf1a1b* 3,  $n = 122$ . PC: WT 1,  $n = 72$ ; WT 2,  $n = 225$ ; WT 3,  $n = 109$ ; *asf1a1b* 1,  $n = 72$ ; *asf1a1b* 2,  $n = 293$ ; *asf1a1b* 3,  $n = 119$ .  $****P < 0.005$  Tukeys multiple comparison test.

(Mougeot et al., 2024). Loss of ASF1 affects neither nuclear shape nor volume, except for GC nuclei, which are larger in two of the *asf1a1b* mutant replicates (Figure S3c). We next quantified the mean chromocenter volume and the relative heterochromatin fraction (RHF), defined as the total chromocenter volume divided by the nuclear volume. In *asf1a1b* plants, both parameters are significantly reduced in PC nuclei and in two GC nuclei replicates (Figure 2f). Altogether, these data reveal that ASF1 is required for *45S rDNA* copy number control and silencing as well as heterochromatin organization.

### ASF1A and ASF1B interact with several members of the H3–H4 histone chaperone network

ASF1 is part of a large histone chaperone network that handles the basic histone proteins from synthesis to deposition, and there are other well-characterized components. To study the interaction of ASF1 with these components, we used a well-established bimolecular fluorescence complementation (BiFC) assay in the Arabidopsis root protoplast system (Kolarova et al., 2021; Nespore Dadejova et al., 2022). We first tested the interaction between ASF1A and ASF1B with HIRA, identified as a major interactor by immunoprecipitation followed by mass spectrometry (IP-MS) (Zhong et al., 2022) and also here by a yeast-2-hybrid (Y2H) screen using ASF1B as bait (Figure 3a; Table S1). In root protoplasts, we confirmed that both ASF1A and ASF1B interact with HIRA in the nucleus (Figure 3b), which corresponds to the results obtained by co-immunoprecipitation (Co-IP) of *in vitro* translated proteins (Figure 3c). Since we noticed that ASF1A, ASF1B, and HIRA can produce false-positive nuclear signals when fused to the C-terminal part of YFP (Figure S4; Table S2), we tested other candidates, namely, NAP1-RELATED PROTEIN 1 (NRP1), and NRP2 (also identified in IP-MS) (Zhong et al., 2022). NRP1 and NRP2 interact with ASF1A and ASF1B in the nucleus and the cytoplasm (Figure S5a,b), confirming the functionality of the BiFC constructs. We also observed that both ASF1A and ASF1B interact with histone H3.1 and H3.3 (Figure 3d), as previously shown by Y2H (Le Goff et al., 2020). We further found that FAS1 interacts predominantly with H3.1 but also occasionally with H3.3 (Table S2), while HIRA binds only H3.3 under these conditions (Figure 3d). In mammals, ASF1A and B bind the p60 subunit of the CAF-1 complex via its B domain (Abascal et al., 2013). While we could not find direct interaction between FAS2 and ASF1A or ASF1B in Co-IP (Figure S5c), we identified FAS2 as an ASF1A and ASF1B interaction partner in Y2H screens (Figure 3a; Table S1) and observed interaction between FAS2 and ASF1B in BiFC (Figure 3e). This suggests that interactions between FAS2 and ASF1 proteins are either weak or only transient (Kerppola, 2008).

### The histone chaperone HIRA is required for telomere and *45S rDNA* maintenance

In mammals, ASF1 protects telomeres from elongation via alternative homologous recombination-based mechanisms, while HIRA promotes telomere elongation (Hoang et al., 2020; Jiang et al., 2011; O'Sullivan et al., 2014). In plants, the contribution of HIRA to telomere length maintenance has not been investigated. We therefore assessed the TRF profile of *hira* mutants and found telomere shortening down to approximately 2.5 kb in length (Figure 4a; Figure S6). Next, we checked whether HIRA is also required for *45S rDNA* copy number regulation. In individual plants from two independent seedling pools, we observed moderately reduced *45S rDNA* amount with variations in *45S rDNA* loss between individual plants and seedling pools (Figure 4b). The reduced copy number observed by quantitative PCR (qPCR) in plants from pool 1 was confirmed by quantification of *45S rDNA* FISH images (Figure 4c,d). We further analyzed *45S rRNA* transcript variants in individual plants of those *hira* mutants for which we examined *45S rDNA* copy number (Figure 4e). We found that similar to *asf1a1b* mutant seedlings, silencing of *45S rRNA VAR1* genes required HIRA (Figure 4e). However, in contrast to *asf1a1b*, differences in telomere length are not accompanied by changes in heterochromatin organization in GC and PC epidermis nuclei in *hira* mutants (Figure 4f; Figure S7). It suggests that defects in the HIRA-mediated replication-independent histone deposition cause less dramatic changes in the nuclear structure and repeat abundance compared to loss of ASF1 proteins.

### Relative nucleosome occupancy at telomeres is not significantly affected in *asf1a1b* and *hira* mutants

Deficiency in histone chaperones disturbs the maintenance of the nuclear histone pool as well as nucleosome assembly, which in turn affects nucleosome occupancy and chromatin organization. We therefore examined whether nucleosome occupancy at telomeric repeats is affected in *asf1a1b* and *hira* mutant plants and performed H3 chromatin immunoprecipitation sequencing (ChIP-seq) in WT, *asf1a1b*, *hira*, and *fas1* mutants. In addition, we included recently published ChIP-seq experiments in WT and *asf1a1b* mutant plants (Zhong et al., 2022) to determine telomere size and to quantify H3 enrichment at telomeric repeats. We initially quantified the number of telomeric repeats in the *asf1a1b*, *hira*, and *fas1* mutant genomes using ChIP input DNA. For this, we determined the ratio of reads mapping to a stretch of five (TTTAGGG)<sub>5</sub> telomere repeats to the reads mapping to the entire genome (Figure 5a). We confirmed reduced telomere length in all three histone chaperone mutants, with the most pronounced reduction observed in *fas1* plants and comparable levels in *asf1a1b* and *hira* mutants, consistent

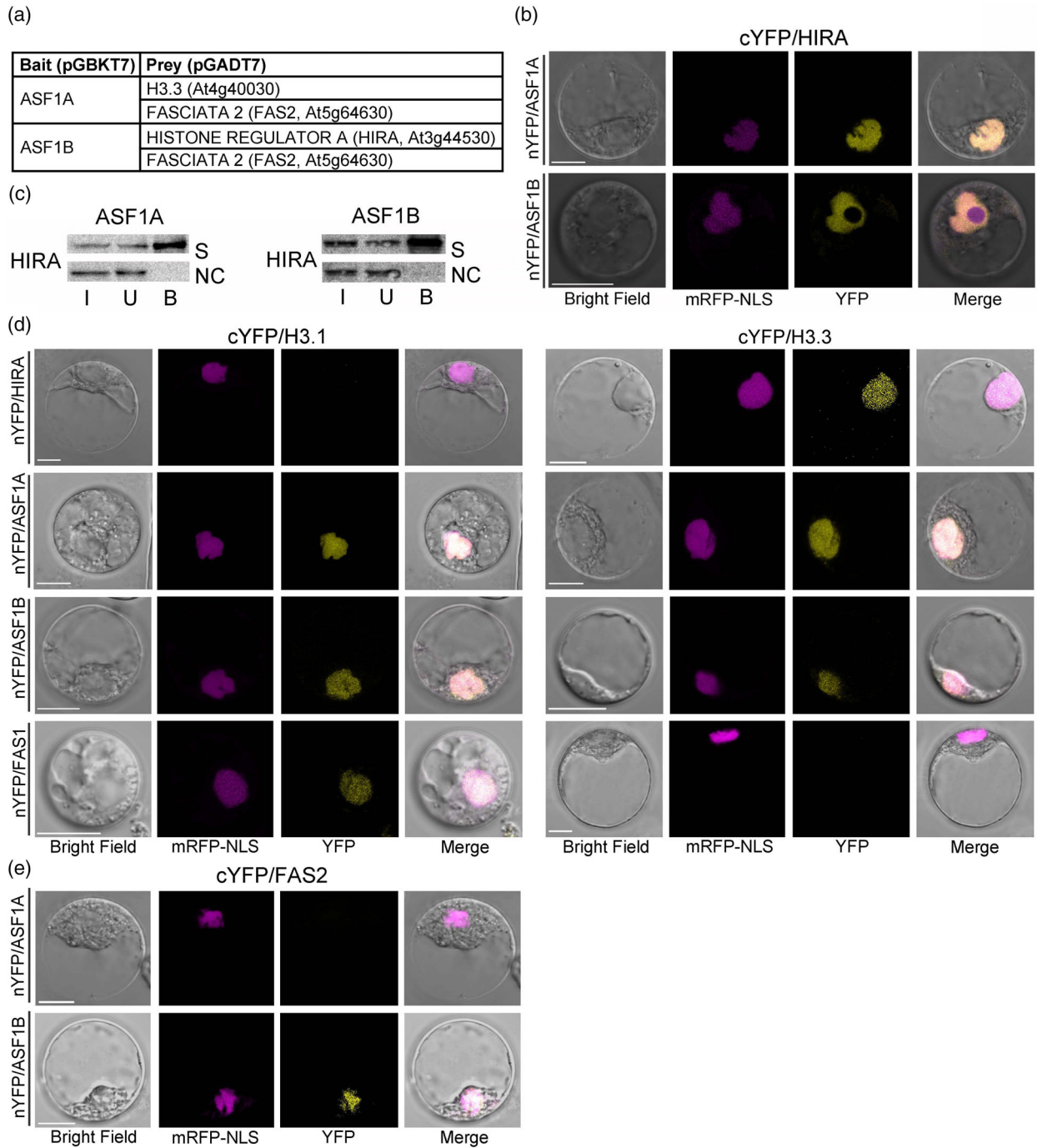


**Figure 3.** ASF1 proteins interact with HIRA, FAS2, and histone variants H3.1 and H3.3.

(a) Interactors identified in a yeast-two-hybrid (Y2H) screen of *Arabidopsis thaliana* cDNA library (prey, pGADT7) with ASF1A or ASF1B as baits (pGBKT7). (b, d, e) Bimolecular fluorescence complementation (BiFC) on protoplasts from root tips of 10-day-old seedlings. Protoplasts were co-transfected with (b) nYFP/ASF1A or nYFP/ASF1B and cYFP/HIRA, (d) nYFP/HIRA, nYFP/ASF1A, nYFP/ASF1B or nYFP/FAS1 with cYFP/H3.1 or cYFP/H3.3, (e) nYFP/ASF1A or nYFP/ASF1B with cYFP/FAS2. Bright field, nuclear localization signal mRFP-NLS (magenta, used as a transformation control), YFP fluorescence (yellow), and the combined images were visualized by confocal microscopy 16 h after transfection. The scale bar represents 10  $\mu$ m. Experiments were repeated twice with similar results. (c) Co-immunoprecipitation analysis (CoIP) of HIRA and ASF1A or ASF1B. Radioactively labeled HIRA with non-labeled Myc-tagged ASF1A or ASF1B was used as a sample (S); in the negative control (NC), no Myc-tagged interaction partner was present. (I) input, (U) unbound, (B) bound.

with the TRF analysis. We then determined the relative H3 occupancy at telomeres in the WT and mutant backgrounds, correcting for the differences in telomere length

in each mutant. Although there was a trend toward reduction in the *asf1a1b* and *hira* mutants, the relative H3 occupancy at telomeres was not significantly different from



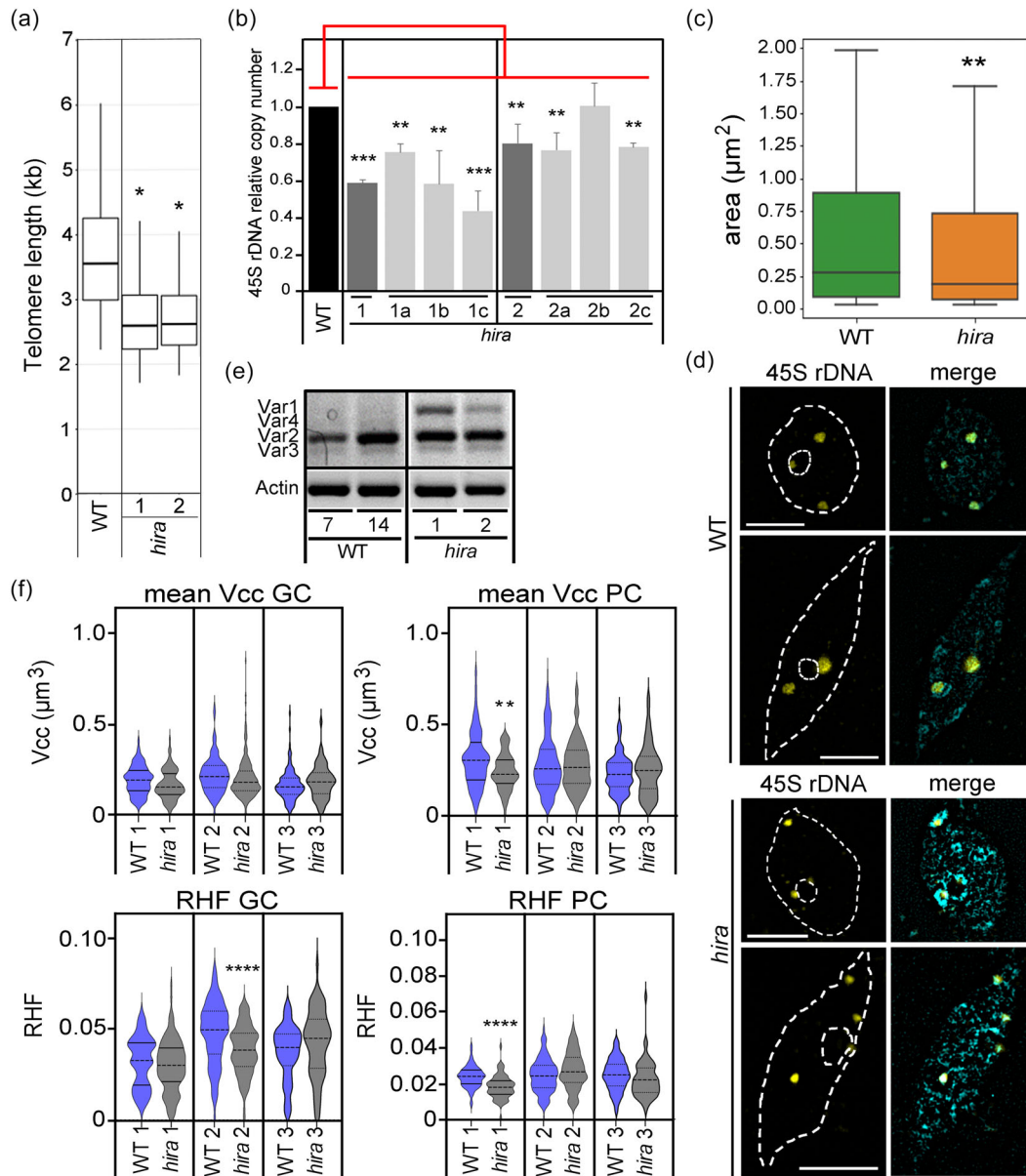


**Figure 4.** Loss of HIRA causes reduced 45S rDNA gene copy number and telomere shortening.

(a) Telomere length in *hira*. Two seedling pools (14-day-old) from independent generations G5 (1) and G7 (2) are shown. Box charts show the first and third quartiles separated by the median value. The maximum and minimum telomere lengths are represented by the whiskers above and under the boxes. \* $P < 0.1$ ,  $t$ -test compared to WT.

(b) 45S rDNA copy number was determined by quantitative PCR (qPCR) in *hira* and WT. For *hira*, two seedling pools (14-day-old) from independent generations G5 (1) and G7 (2) and individual sister plants (5-week-old leaves, 1a–c and 2a–c) are shown. Relative 45S rDNA copy number, with WT set to 1 and using *UBLQUITIN 10* as a reference, is shown. \*\*\*\* $P < 0.01$ , \*\* $P < 0.05$  compared to WT, two-sided  $t$ -test.

(c) Quantification of the signal area of 45S rDNA signals obtained by fluorescence *in situ* hybridization (FISH) with consequent super-resolution microscopy (2D SIM) on nuclei of 10-day-old seedlings in WT and *hira* (G5). One hundred nuclei of WT and *hira* were hybridized with the 45S rDNA probe. Box charts show the first and third quartiles separated by the median value. The maximum and minimum values are represented by the whiskers above and under the boxes. \*\* $P < 0.05$ ; compared to WT, Kruskal–Wallis test.

(d) 45S rDNA localization pattern obtained by fluorescence *in situ* hybridization (FISH) with consequent super-resolution microscopy (2D SIM) on nuclei of 10-day-old WT and *hira* seedlings. Approximately 100 nuclei of WT and *hira* mutant seedlings were probed with a 45S rDNA probe (yellow) and DNA counterstained with DAPI (blue). Dashed lines indicate the contours of nuclei and nucleoli. The scale bar represents 5 µm. Note that images of the WT nuclei are the same as in Figures 1f and 2a.

(e) Reverse transcription followed by PCR (RT-PCR) amplification of 45S rDNA variants in 14-day-old *hira* mutant seedlings compared to 7-day and 14-day-old WT seedlings. Two independent generations G5 (1) and G7 (2) of *hira* were analyzed.

(f) Quantification of mean chromocentre volume (Vcc) and relative heterochromatin fraction (RHF) in GC and PC of three independent biological replicates. GC: WT 1,  $n = 193$ ; WT 2,  $n = 189$ ; WT 3,  $n = 154$ ; *hira* 1,  $n = 115$ ; *hira* 2,  $n = 194$ ; *hira* 3,  $n = 64$ . PC: WT 1,  $n = 72$ ; WT 2,  $n = 225$ ; WT 3,  $n = 134$ ; *hira* 1,  $n = 67$ ; *hira* 2,  $n = 160$ ; *hira* 3,  $n = 59$ . \*\*\*\* $P < 0.005$ ; \*\* $P < 0.05$  Tukeys multiple comparison test.

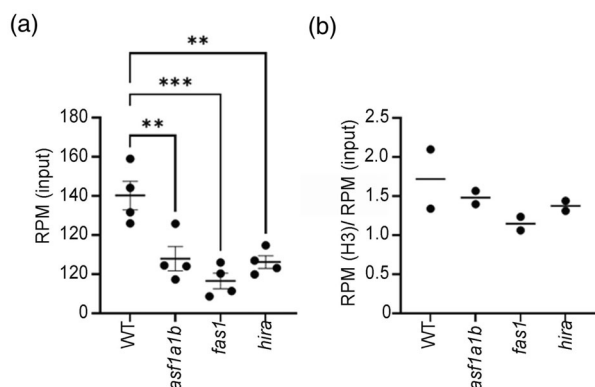


**Figure 5.** Relative H3 occupancy at telomeres is unchanged in histone chaperone mutants.

(a) Abundance of telomeric repeats and (b) relative H3 occupancy at telomeres are shown as RPM (reads containing telomere sequences per million reads mapped to the genome) in WT and *asf1a1b*, *fas1*, and *hira* mutants. H3 ChIP data were normalized by the relative number of telomeric reads in the respective inputs as determined in (a). Four replicates for the input (a) and two replicates for the H3-ChIP (b) were used for each genotype. \*\*\* $P < 0.01$  and \*\* $P < 0.05$  compared to WT, ANOVA one way and Dunnett's test.

that of wild type (Figure 5b; Figure S8). We conclude that loss of either HIRA or ASF1 does not specifically affect nucleosome occupancy at telomeres.

#### ASF1 and HIRA interact with telomere-associated proteins *in vivo*

Telomere stability is defined by interactions with telomere-specific proteins and general chromatin-binding factors (Fulneckova et al., 2021; Kolarova et al., 2021; Schorova et al., 2019; Schruppova et al., 2014). Since the list of ASF1B interactors (Zhong et al., 2022) included selected telomere candidates, namely, dyskerin, TRB1, TRB3 (three components of the putative *Arabidopsis* protective telomere complex, Schruppova et al., 2019), we next addressed whether ASF1 could be directly interacting with telomere protein complexes *in vivo*, specifically testing telomerase and TRB1. Our experiments revealed ASF1A and TRB1 interactions in the nucleus and nucleolus (Figure 6a; Table S3). Interestingly, we found that the ASF1–TRB1 interaction is modulated in *hira* or *fas1* mutant backgrounds, where these ASF1 binding partners are lacking. In the *hira* or *fas1* mutant context, TRB1 interacts with both ASF1A and ASF1B predominantly in the nucleolus (Figure 6b,c). Finally, to test the interaction with telomerase, we used two N-terminal fragments (RID with a nuclear localization sequence [NLS] and TEN without this motif) that both localize to the nucleus and the nucleolus (Zachova et al., 2013). Notably, ASF1A and ASF1B bind to RID (Figure 6d) but not to TEN (Figure S9a), indicating that the lacking part of the telomerase protein in TEN is required for histone chaperone binding. Additionally, using

available ChIP-seq data (Zhong et al., 2022), we confirmed the enrichment of ASF1A and ASF1B at telomeric DNA (Figure S9b).

In conclusion, our results indicate the existence of a complex of histone chaperones and telomere proteins potentially held together by telomerase interacting with ASF1A. Furthermore, the interaction between ASF1 and the RID version of the telomerase establishes a physical link between the chaperone and the telomere maintenance enzyme and could explain the requirement of ASF1 proteins in telomere length homeostasis.

## DISCUSSION

### ASF1 interacts with members of the histone chaperone network

Precise chromatin assembly, mediated by histone chaperones, profoundly influences genome organization at multiple levels, including the regulation of gene expression, site-specific silencing, and the formation of heterochromatin (Anderson et al., 2009; Benoit et al., 2019; Ono et al., 2006; Sharp et al., 2001), or long-distance genome associations (Feng et al., 2022; Picart-Piccolo et al., 2020). To achieve these different functions, histones are handled by a network of histone chaperones for deposition, eviction, or recycling during replication and transcription (Typas, 2023). *Arabidopsis* ASF1 is involved in multiple interactions within this network. Using BiFC, Y2H, and Co-IP, we find that ASF1 interacts with HIRA, consistent with previous observations from mass spectrometry (Zhong et al., 2022). We also found interactions between ASF1 and FAS2 by BiFC and identified FAS2 as bait in an Y2H screen. Since FAS2 was not detected by mass spectrometry (Zhong et al., 2022), this suggests rather transient interactions between ASF1 and the CAF-1 complex (Kerppola, 2008; Miller et al., 2015), consistent with previous observations in mammals where interaction between human ASF1 and CAF-1 is frail and lost upon high salt washes (Klimovskaia et al., 2014). Though the BiFC system is excellent for detecting even weak interactions, if they occur in a short time window, they may still evade detection – a possible scenario for FAS1-ASF1B. In addition, we reveal interactions with NRP1 and NRP2, demonstrating that ASF1 can interact with several players of the histone chaperone network either directly or mediated by histone contacts.

### ASF1 deficiency causes telomere instability

Telomere length is reduced in both *asf1a1b* and *hira* plants, establishing that both histone chaperones are required for reliable maintenance of telomere length in *Arabidopsis*. Consistent with the plant phenotypes of the respective genotypes, telomere defects only occur in the *asf1a1b* double mutant but not in single mutants, and

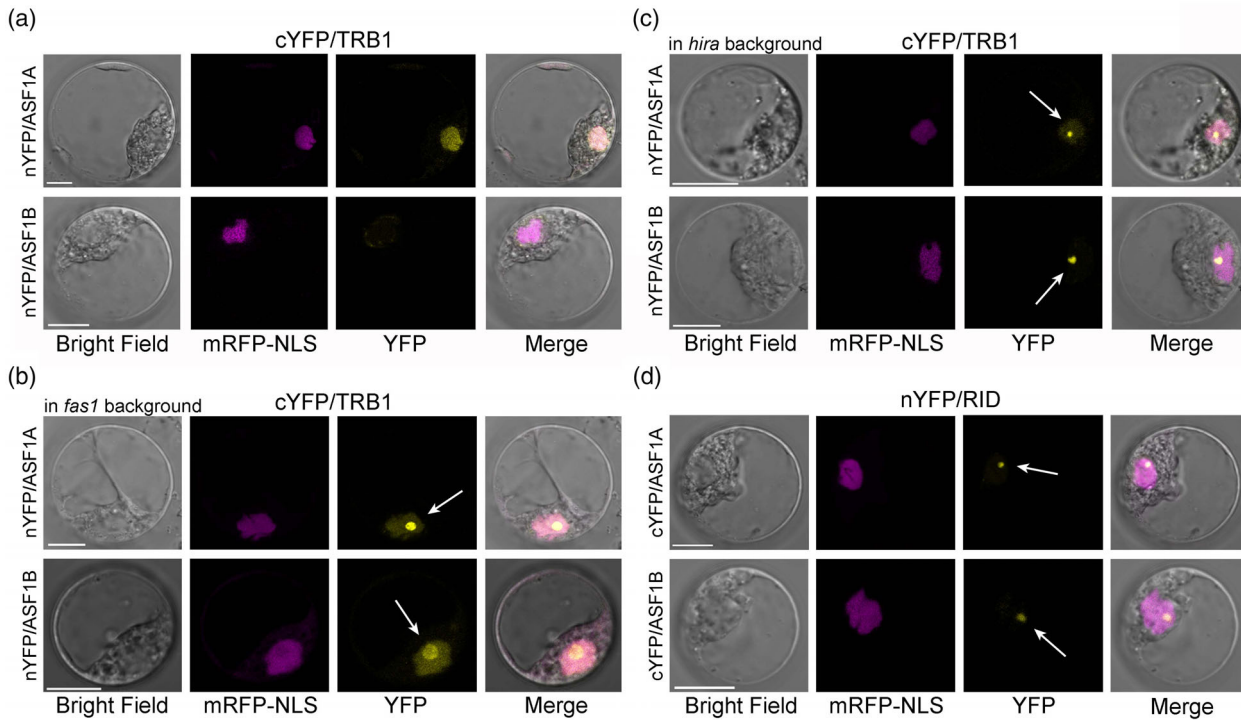


**Figure 6.** ASF1A and ASF1B interact with TRB1 and telomerase.

(a–d) Bimolecular fluorescence complementation (BiFC) in protoplasts from root tips of 10-day-old seedlings. Protoplasts were co-transfected with (a–c) nYFP/ASF1A or nYFP/ASF1B and cYFP/TRB1, (d) nYFP/RID with cYFP/ASF1A or cYFP/ASF1B plasmids. Bright field, nuclear localization signal mRFP-NLS (magenta, used as a transformation control), YFP fluorescence (yellow), and the combined images were visualized by confocal microscopy 16 h after transfection. White arrows indicate protein–protein interactions in the nucleolus. The scale bar represents 10  $\mu\text{m}$ . Experiments were repeated twice with similar results.

deletion of either ASF1A or ASF1B in a *fas* mutant background does not exacerbate telomere defects. This strongly suggests that ASF1A and ASF1B act redundantly in telomere length regulation and that they can compensate for each other's function even in the sensitized mutant background for CAF-1, which is already affected in the replication-dependent histone assembly pathway. Contrary to findings in yeast, where the depletion of ASF1 leads to telomere mis-localization without affecting telomere length (Hiraga et al., 2008), the majority of telomeres are localized near the nucleolus in *asf1a1b* as in WT, but telomeres are shorter. Upon depletion of ASF1, mammalian cell lines exhibit rapid initiation of the alternative telomere lengthening (ALT) pathway, associated with telomere elongation and downregulation of telomerase expression (O'Sullivan et al., 2014), which also contrasts with the telomere defects in *asf1a1b*. Thus, distinct from the conserved role of ASF1 in histone handling, our findings contribute to the emerging picture revealing functional divergence of ASF1's roles in telomere maintenance in plant, yeast, and mammalian models.

In mammals, a dedicated histone chaperone complex, DEATH DOMAIN-ASSOCIATED PROTEIN (DAXX) and the ALPHA-THALASSEMIA/MENTAL RETARDATION SYNDROME X-LINKED PROTEIN (ATRX) (Goldberg et al., 2010; Lewis

et al., 2010), mediates chromatin assembly at telomeres and centromeres. When ATRX is depleted in mammals, HIRA is recruited to telomeres to enhance ALT and to form ALT-associated bodies (Hoang et al., 2020; Jiang et al., 2011). Loss of ATRX in plants causes reduced H3.3 levels and impacts *45S rRNA* expression (Duc et al., 2017); however, whether it plays a role in telomere maintenance in plants and cooperates with ASF1 remains to be explored. Given the unique composition of telomeric chromatin, and signs of transcriptional activity initiated within genes near telomeres (Vrbsky et al., 2010), it is reasonable to suggest that a functional chromatin configuration at chromosome ends depends on the coordinated efforts of several histone deposition and recycling pathways. The observation that the absence of ASF1 or HIRA does not result in significant changes in relative H3 occupancy at telomeres may also suggest a possible modulation of the balance between individual histone variants, as previously demonstrated (Kolarova et al., 2021; Zhong et al., 2022).

#### A general role for ASF1 in genome stability and heterochromatin organization

Apart from the prominent effect of ASF1 on telomere length, we noticed that the loss of ASF1 leads to *45S rDNA* instability with a reduction in *45S rRNA* gene copy number

and reactivation of the normally silent *VAR1 45S rRNA* genes localized on NOR2 (Chandrasekhara et al., 2016). In line with this observation, we also find that heterochromatin organization is more generally affected upon loss of ASF1, as the mean volume of chromocenters, which represent clusters of centromeric, pericentromeric, and *rDNA* (Fransz et al., 2002; Probst et al., 2003), is significantly reduced. Histone chaperones are crucial for chromocenter formation (Arakawa et al., 2015; Guthmann et al., 2023), for example, the altered histone deposition in *fas2* mutants leads to aberrant heterochromatin clustering and accumulation of H3.3 in chromocenters that are normally enriched in H3.1 (Benoit et al., 2019; Otero et al., 2016). Similarly, yeast histone chaperone mutants often show reduced transcriptional silencing (Huang et al., 2007; Sharp et al., 2001; Wu et al., 2017). Yeast ASF1 is enriched at telomeres, centromeres, and *rDNA* (Dewari & Bhargava, 2014), and we see the association of ASF1 with telomeres also in Arabidopsis. Similarly, Drosophila ASF1 physically associates with heterochromatin at centromeres (Moshkin et al., 2002). Whether the reduced heterochromatin fraction results from a defect in the clustering of the repeats or a reduction in the number of centromeric repeats or transposons remains to be investigated. Mutants in HIRA have defects in *45S rDNA* silencing as well as heterogeneity in *45S rRNA* gene copy number, but chromocenter volumes are unaffected, in contrast to *asf1a1b*. This indicates that, at repetitive sequences, ASF1 may have a function beyond facilitating HIRA-mediated deposition, possibly linked to the replicative chromatin assembly via the CAF-1 complex.

### Telomeres, DNA damage hotspots during DNA and chromatin replication

Telomere length homeostasis is maintained through the coordinated actions of telomerase (Fajkus et al., 1998; Greider & Blackburn, 1985, 1996), telomere-specific complexes that recruit telomerase to chromosomal ends, thereby preventing misidentification of these regions as DNA break sites (Palm & de Lange, 2008; Timashev et al., 2017) and telomerase-independent processes (Riha et al., 2001; Ruckova et al., 2008). Here, we show that, in Arabidopsis, depletion of ASF1 and HIRA causes telomere shortening, adding to the previous work on *caf-1* mutants (Mozgova et al., 2010). Based on the rate of telomere shortening in these different mutant contexts, we hypothesize that the underlying molecular mechanisms differ. In Arabidopsis mutants lacking telomerase (*tert*), the rate of erosion equals 250–600 base pairs per generation, as the failure to fully replicate the lagging strand of the telomere is not corrected by telomerase (Riha et al., 2001). Telomerase activity is unaffected in *asf1a1b* mutants; moreover, neither *asf1a1b* nor *hira* plants show progressive telomere erosion. In *fas1*, telomere loss is progressive (Mozgova et al., 2010), yet, telomerase independent (Jaske

et al., 2013; Mozgova et al., 2010). It rather involves the NAP1 histone chaperone (Kolarova et al., 2021) and DNA repair kinase ATAXIA TELANGIECTASIA MUTATED (ATM) (Eekhout et al., 2021). Therefore, the mechanism of telomere erosion in histone chaperone mutants may not include regulation of the enzyme processivity but may be linked to the reparative processes. For example, in *fas1*, the G1/S checkpoint is overridden in favor of G2/M signaling, and *fas1* mutants show a continuous activation of DNA repair genes (Eekhout et al., 2021; Exner et al., 2006; Kolarova et al., 2021). The observation that ATM deficiency does not cause telomere reversion in *tert* (Vespa et al., 2007) indicates that the reparative processes activated in *fas1* are likely stimulated by defects arising upon replication. In mammals, ASF1 supports the process of non-homologous end joining at telomeres, being directed to dysfunctional telomeres via RIF1 (RAP1-interacting factor homolog) (Silverman et al., 2004; Tang et al., 2022). The function of the ASF1–RIF1 complex in DNA damage repair is distinct from the histone chaperone activity of ASF1, indicating the potentially diverse functions of this histone chaperone (Tang et al., 2022).

A similar situation occurs in Arabidopsis *asf1a1b* mutants that display S phase arrest, upregulation of repair genes, and accumulation of damaged DNA (Zhu et al., 2011). Unlike *fas1* mutants, both cell cycle checkpoints are active in *asf1a1b* mutants, as evidenced by their sensitivity to hydroxyurea (Eekhout et al., 2021; Zhu et al., 2011). Telomeres, as well as *45S rDNA*, are particularly susceptible to changes in chromatin composition and represent challenging templates for replication (Dvorackova et al., 2015; Wu et al., 2021). Deficient histone recycling or *de novo* deposition of H3 variants at the replication fork results in altered chromatin characteristics and may impact replication timing, thereby increasing the susceptibility to DNA breaks (Klein et al., 2021). Such a direct role for chromatin maturation in influencing DNA repair at replication forks has been recently shown for the recruitment of the DNA repair protein TONSOKU that is recruited via interaction with unmodified H3.1 tails but released upon chromatin maturation including methylation of the histone tail (Davarinejad et al., 2022). Therefore, one way how ASF1 might prevent erosion of telomeres is by preventing DNA damage and allowing efficient repair through controlled histone recycling and *de novo* deposition.

### Evidence for direct interaction between ASF1 and the telomere maintenance/protection machinery

Beyond its role in histone handling, ASF1 may contribute to telomere maintenance by directly interacting with telomere proteins (Zhong et al., 2022). Indeed, we found evidence that ASF1 interacts with the N-terminal domain of telomerase. This interaction might be transient and only occur *in vivo* at telomere sites. Telomerase (TERT) also

interacts with the Arabidopsis NAP1 histone chaperones within the nucleus and nucleolus (Fulneckova et al., 2021) and with MCM5 of the MCM helicase complex (Fulneckova et al., 2021). Notably, the mammalian MCM helicase complex has also been shown to interact with ASF1 via a histone bridge (Groth et al., 2007). The nucleolus has been discussed to be a possible location for telomerase assembly (Schrumppova et al., 2019), and the telomere positioning around the nucleolus has been linked to their size control in Arabidopsis (Pontvianne et al., 2016). Chromatin assembly, replication, and DNA repair may therefore occur in close association with the nucleolus, where the telomerase RNA-binding protein dyskerin and TERT gather (Kannan et al., 2008; Lermontova et al., 2007). Finally, according to ChIP-seq data (Zhong et al., 2022), ASF1 is enriched at telomere sequences.

We also observe the interaction of ASF1 with TRB1, a nuclear protein found in both the nucleus and the nucleolus that binds telomere repeats via its Myb domain (Dvorackova et al., 2010). TRB1, similarly to RAP1 or RIF1, is not a telomere-exclusive protein (Schrumppova et al., 2016; Teano et al., 2023; Zhou et al., 2016). We find more nuclei showing ASF1B–TRB1 interactions in *hira* and *fas1* mutant plants, where interactions occur preferentially in the nucleolus. Similarly, the ASF1A–TRB1 complex is more often found in the nucleolus in mutant backgrounds, suggesting that alternative complexes are formed at least transiently when conserved histone chaperones are missing. The functional relevance of these interactions between ASF1 and telomere proteins needs to be further tested, but the data strongly suggest that ASF1 plays an indirect role at telomeres through the maintenance of chromatin organization as well as a more direct role through interaction with telomere maintenance proteins.

## EXPERIMENTAL PROCEDURES

### Plant material and growth conditions

*Arabidopsis thaliana* ecotype Columbia-0 was used as a WT; all mutants are the previously described T-DNA insertion lines: *fas1-4* (SAIL\_662\_D10) (Mozgova et al., 2010); *fas2-5* (SALK\_147693) and *hira* (WiscDsLox362H05) (Duc et al., 2015); *asf1a-2* (GK-200G05) and *-asf1b-1* (SALK\_105822) (Zhu et al., 2011). *asf1a-2*, *asf1b-1*, and *asf1a1b* seeds were kindly provided and described by Zhu et al. (2011). Double mutants *asf1a fas1*, *asf1b fas1*, *asf1a fas2*, and *asf1b fas2* were obtained by crossing. F2 progeny from heterozygous F1 plants was genotyped for the respective allele combinations (Tables S4 and S5) and then propagated into F3–F6 consecutive generations. All seeds were surface-sterilized (75% ethanol/5 min and then 96% ethanol/5 min) and plated on half-strength agar Murashige and Skoog medium (½ MS medium) with 1% sucrose. After 2 days of stratification (4°C/dark), plants were grown in a growth chamber under short-day (SD) conditions (8 h light – 21°C; 16 h dark – 19°C; 50–60% relative humidity) and for *biom3D* image analysis under long-day conditions (16 h light/8 h dark). Seedlings were transferred into soil 2 weeks after germination and were grown under the same illumination and temperature conditions.

### DNA isolation and plant genotyping

DNA for TRF from 5-week-old rosette leaves or 14-day-old seedlings was isolated according to Dellaporta et al. (1983) with minor changes (see Data S1). For genotyping, DNA was isolated using a modified protocol (Edwards et al., 1991) or GenElute Plant Genomic DNA Miniprep Kits (MERCK, Rahway, NJ, USA) according to the manufacturer's instructions. DNA concentration was determined using Qubit (Thermo Fisher Scientific) or NanoDrop2000 (Thermo Fisher Scientific, Waltham, MA, USA) systems. One microlitre of DNA was used in a PCR reaction using 0.3 μM primers and 5 U of MyTaq™ Red DNA Polymerase (Bioline, Memphis, TN, USA). Primers are listed in Tables S4 and S5.

### TRF analysis

Telomere length was determined with total DNA isolated from 5-week-old rosette leaves or 14-day-old seedlings as described (Kolarova et al., 2021). TRF signals were visualized using a Typhoon FLA-7000 imaging system (Fuji film) and evaluated using the WALTER toolset (Lycka et al., 2021). Statistically significant differences between two groups of mutants or two WT were determined using a two-tailed Welch's *t*-test.

### Telomere repeat amplification protocol

TRAP assays for plant telomerase activity were performed on 10-day-old seedlings as described previously (Fitzgerald et al., 1996). For more details, see Data S1.

### Slide preparation and FISH

Root nuclei from 3-week-old *A. thaliana* seedlings were isolated and processed as described in Data S1. FISH was performed as described (Zavodnik et al., 2023). We used a custom LNA telomeric (TTTAGGG<sub>3</sub> – Alexa Fluor 488) and biotin-labeled *45S rDNA* probe, prepared with nick-translation of the T15P10 BAC covering *45S rDNA* (10 nm final concentration for both probes). Slides were covered with a glass coverslip and sealed with rubber cement, denatured together with probes at 80°C for 3 min, and hybridized overnight in a humid chamber at 37°C. Post-hybridization washing steps included 3 × 5 min in 50% formamide/2 × 5 min in 2 × SSC at 42°C and 2 × 5 min in 2 × SSC at room temperature. Chromosomes were counterstained with 4,6-diamidino-2-phenylindole (DAPI; 1 mg ml<sup>-1</sup>) in Vectashield (Vector Laboratories). Structured illumination microscopy was performed on the Zeiss Elyra 7 super-resolution microscopy system, using a 63× oil plan-apochromat objective and the corresponding filter cubes (DAPI, Alexa Fluor 488, and Texas Red). SIM image reconstruction was performed in batch using the built-in Zeiss proprietary SIM reconstruction algorithm in Zen Blue 3.0.

### Image analysis and statistical analysis

After SIM image reconstruction, images were processed by background subtraction using the same threshold for all samples. Telomeric and *45S rDNA* spots were analyzed in Imaris 10 software (Bitplane, Oxford). Signals were automatically discriminated by the object detection algorithm and manually checked for possible artifacts (Figure S10a). Only the spots inside plant nuclei were selected to export volume (or area) and intensity. Statistical tests were performed in the SciPy Python library. Statistical differences between WT and mutants or between groups were determined using the Kruskal–Wallis and Wilcoxon rank-sum tests, respectively. Most analyzed nuclei showed an elongated shape, with the average number of spots per nucleus close to 7.5 for telomeres and 2.5 for *45S rDNA*, indicating similar ploidy (Figure S10b).

## Nuclear morphology and chromatin organization analysis

Cotyledons from 10-day-old (replicates 1 and 2) and 14-day-old (replicate 3) WT, *asf1a1b*, and *hira* seedlings were prepared as previously described (Desset et al., 2018), DNA stained overnight with Hoechst (Hoechst 33258 at 1  $\mu\text{g ml}^{-1}$  final concentration) and cotyledons mounted in PBS:glycerol (20:80). Microscopic observations were performed as described in Desset et al. (2018), and 3D images containing one single nucleus were obtained using the *NucleusJ* 2.0 auto-crop option (Dubos et al., 2020). Each epidermal nucleus was assigned to either guard cells or pavement cells after combining a maximum Z-projection of a wide-field stack and a single plane image under transmission light using differential interference contrast. Nuclear morphology and chromocenter volume were obtained using the deep learning Python package *biom3D*, an in-house developed deep learning tool for volumetric image segmentation (<https://github.com/GuillaumeMougeot/biom3d>). In short, *biom3d* was used to train deep learning models on image datasets of Arabidopsis nuclei, for which the nuclear volume ( $N = 103$ ) and the chromocenters ( $N = 85$ ) were segmented manually using the Napari software. Two separate models, one to segment nuclear volume and the other to segment chromocenters, were generated. All segmentation predictions were verified by eye after overlay with the respective raw image, and obviously aberrant predictions were discarded. Quantitative parameters were subsequently extracted from the resulting segmentations.

## Quantitative PCR

For the relative quantification of *45S rDNA* copy number, total DNA from 4- or 5-week-old leaves from a single plant or a mix of 14-day-old seedlings was used. qPCR was performed according to standard procedures using SensiFAST™ SYBR® Hi-ROX (Meridian Bioscience) and a combination of primers for *18S rDNA* (226 bp long product) normalized to *UBIQUITIN 10* (see Tables S4 and S5). The analysis was performed by StepOnePlus Real-Time PCR system (Applied Biosystems) under the following conditions: 95°C/3 min; 35 cycles of 95°C/5 sec, 60°C/20 sec, 72°C/10 sec, and 72°C/1 min followed by standard melting analysis. Reactions for each sample were carried out in technical triplicates in leaves of three independent biological replicas (*asf1a1b*) or leaves or seedlings from two independent *hira* mutant seed batches. Standard deviation visualizes the variability among technical replicas. The *t*-test was used for statistical evaluation when comparing the copy numbers of mutants and WT controls.

## Cloning

Cloned sequences used for protein–protein interaction studies (BiFC, Y2H, and Co-IP) were *FAS1*, *FAS2*, *ASF1A* (see Kolarova et al., 2021), *TRB1* (Schrumpfova et al., 2014), *RID*, *TEN* (see Zachova et al., 2013). The remaining genes were cloned according to Kolarova et al. (2021). For more details, see Data S1.

## Co-IP and yeast-2-hybrid screen

Co-IP was performed *in vitro* according to Schrumpfova et al. (2014) and Kolarova et al. (2021). Yeast-2-Hybrid screening using *ASF1A* and *ASF1B* as baits was performed as in Le Goff et al. (2020). See Data S1 for details.

## Bimolecular fluorescence complementation

To prepare protoplasts, the roots of 7-day-old seedlings were chopped with a razor blade and processed according to Kolarova

et al. (2021). Fluorescence signals were observed using a Zeiss LSM 800 laser scanning confocal microscope with YFP (Alexa Fluor 488) and RFP (Texas Red) filters, equipped with Plan-Apochromat 63 $\times$ /1.40 water objective. For image analysis and contrast enhancement, ZEN 2.5 lite blue edition software was used.

## H3 ChIP-seq and bioinformatic data processing

ChIP-seq experiments were performed as described by Song et al. (2014) using 1 g of 3-week-old WT, *asf1a1b*, *hira*, and *fas1 in vitro*-grown seedlings. Chromatin was sheared using the COVARIS system in 130  $\mu\text{l}$  Covaris microTubes (Intensity: 5, Duty cycle: 15%, Cycles/burst: 300, Duration: 420 sec, Mode: frequent sweeping) and spiked with 10% of chromatin from *Drosophila* S2 cells. ChIP-seq libraries were generated using the NEBNext® Ultra™ II DNA Library Prep Kit for Illumina® (New England Biolabs) from 10 ng of starting material. Sequencing was performed on a HiSeq2500, with paired-end reads of 50 bp lengths, quality checked by FASTQC and mapped to *Drosophila* and Arabidopsis reference genomes (Table S6). To estimate differences in telomere length, reads from input samples from this study and from Zhong et al. (2022) (PRJNA779072) were mapped to five consecutive telomere repeats (TTTAGGG)<sub>5</sub> using Computel (Nersisyan & Arakelyan, 2015) and normalized to the total number of reads mapping to the Arabidopsis genome (Naish et al., 2021) with the same alignment options used by Computel (bowtie2 --end-to-end --phred33 --n-ceil 38 -D 20 -R 3 -N 1 -L 16 -i S,1,0.5) (Langmead et al., 2009). To determine relative H3 occupancy at telomere repeats, the same procedure was applied, and ratios were corrected for measured telomere length in the respective mutants. ASF1-ChIP-seq signals (PRJNA779072 data set) were processed using an established ChIP-seq pipeline and analyzed for telomere repeats; see Data S1 for details.

## Expression of 45S rDNA variants

Expression analysis of rRNA variants was performed using 7- and 14-day-old WT as control and 14-day-old mutant seedlings according to established protocols (Pontvianne et al., 2013); see Data S1 for details.

## ACCESSION NUMBERS

FAS1 (At1G65470), FAS2 (At5G64630), ASF1A (At1G66740), ASF1B (AT5G38110), HIRA (At3g44530), TRB1 (At1G49950), RID and TEN (both At5G16850), NRP1 (At1G74560), NRP2 (At1G18800), H3.1 (At5G10400), and H3.3 (At4G40040).

## AUTHOR CONTRIBUTIONS

MD and AVP provided ideas and the concept for the project and obtained funding. AM performed the majority of the experimental work, data analysis, and preparation of the figures. CD generated some of the original plant material, SLG performed Y2H screens with AM, and JB carried out ChIP-seq. MD, JS, and LS performed the bioinformatic analysis. GM developed *Biom3D*; SD and AVP performed *biom3D* image analysis. MND participated in BiFC and co-IP experiments; MF contributed to the telomere and *45S rDNA* FISH; MD participated in TRF and NGS-data analysis. MD, AVP, and AM wrote the manuscript with input from MND.

## ACKNOWLEDGMENTS

This work was supported by the Czech Science Foundation project 23-06643S (MD, AM, MND, MF), Grant Agency of Masaryk University project no. MUNI/R/1364/2023, project TowArds Next GENeration Crops, reg. no. CZ.02.01.01/00/22\_008/0004581 of the ERDF Programme Johannes Amos Comenius, the French National Research Agency, grants “Dynam’Het” ANR-11 JSV2 009 01 and “SeedChrom” ANR-22 CE20 0028. We would like to thank Jana Kapustova and Monika Chropovska for their excellent technical support. The Plant Sciences, Cellular Imaging, and Bioinformatics core facilities of CEITEC MU are gratefully acknowledged as well as the iGReD CLIC microscopy facility and the 16-IDEX-0001 CAP 20-25 challenge 1. We thank Wen-Hui Shen (CNRS, Strasbourg, France) for providing us with seeds, Miloslava Fojtová (CEITEC MU, Brno, CR) for performing TRAP assays, Martin Lyčka (NCBR, MU, Brno, CR) for statistical analysis of TRF assays, Ortrun Mittelsten Scheid (GMI, Vienna, Austria) for access to the ChIP-seq experiments performed in her laboratory and critical reading of the manuscript, and Israel Ausin and Zhenhui Zhong (Northwest A&F University, Yangling Shaanxi, China) for providing the details on the H3 and ASF1 ChIP-seq data. We acknowledge the Mobility Program Erasmus+, PHC Barrande (MEYS 8J20FR022), and the COST-Action INDEPTH (CA16212) for networking and travel funds.

## CONFLICT OF INTEREST

The authors declare no conflict of interest.

## DATA AVAILABILITY STATEMENT

The authors responsible for the distribution of materials integral to the findings presented in this article are Martina Dvorackova ([martina.dvorackova@ceitec.muni.cz](mailto:martina.dvorackova@ceitec.muni.cz)) and Aline V. Probst ([aline.probst@uca.fr](mailto:aline.probst@uca.fr)). Raw images, datasets for training, and predictions are available here: <https://omero.bio.fsu.edu/webclient/?show=project-4901>. Models are attached to their training datasets. The associated script can be accessed at <https://github.com/GuillaumeMougeot/biom3d>. Input and H3 ChIP-seq datasets correspond to Bioproject PRJNA1131763.

## SUPPORTING INFORMATION

Additional Supporting Information may be found in the online version of this article.

**Figure S1.** Telomeres in the *asf1a1b* double mutant are shortened without disruption of telomerase activity.

**Figure S2.** Telomere length in *fas1* or *fas2* mutants deficient for ASF1A or ASF1B.

**Figure S3.** *asf1a1b* double mutants show no chromosomal aberrations and globally unaffected nuclear volume and sphericity except for larger nuclear volume in guard cells.

**Figure S4.** Control experiments for protein–protein interaction tests by bimolecular fluorescence complementation.

**Figure S5.** ASF1 proteins interact with NRP histone chaperones.

**Figure S6.** Telomere length in *hira* single mutants.

**Figure S7.** Nuclear volume and shape are unchanged in GC and PC epidermis nuclei in *hira* mutants compared to WT.

**Figure S8.** H3 occupancy at telomeres in *asf1a1b* plants compared to WT.

**Figure S9.** ASF1 and HIRA proteins do not interact with TEN, but ASF1 is present at telomeres.

**Figure S10.** Evaluation of the telomere/45S rDNA signals in WT and *asf1a1b* mutant nuclei obtained by super-resolution microscopy (2D SIM) using Imaris software.

**Table S1.** List of interacting proteins identified in an Y2H screen using ASF1A and ASF1B as baits.

**Table S2.** BiFC experiments of histone chaperone proteins, empty vectors, and H3 variants.

**Table S3.** BiFC experiments of histone chaperones with telomeric proteins.

**Table S4.** List of primers.

**Table S5.** Primer combinations.

**Table S6.** Percentage of reads mapping to Drosophila and Arabidopsis genomes in Drosophila-spiked WT, *asf1a1b*, *hira* and *fas1* input, and ChIP-seq datasets.

**Data S1.** Experimental procedures.

## REFERENCES

- Abascal, F., Corpet, A., Gurard-Levin, Z.A., Juan, D., Ochsenbein, F., Rico, D. *et al.* (2013) Subfunctionalization via adaptive evolution influenced by genomic context: the case of histone chaperones ASF1a and ASF1b. *Molecular Biology and Evolution*, **30**, 1853–1866.
- Adam, S., Polo, S.E. & Almouzni, G. (2013) Transcription recovery after DNA damage requires chromatin priming by the H3.3 histone chaperone HIRA. *Cell*, **155**, 94–106.
- Anderson, H.E., Wardle, J., Korkut, S.V., Murton, H.E., Lopez-Maury, L., Bahler, J. *et al.* (2009) The fission yeast HIRA histone chaperone is required for promoter silencing and the suppression of cryptic antisense transcripts. *Molecular and Cellular Biology*, **29**, 5158–5167.
- Arakawa, T., Nakatani, T., Oda, M., Kimura, Y., Sekita, Y., Kimura, T. *et al.* (2015) Stella controls chromocenter formation through regulation of Daxx expression in 2-cell embryos. *Biochemical and Biophysical Research Communications*, **466**, 60–65.
- Armstrong, S.J., Franklin, F.C. & Jones, G.H. (2001) Nucleolus-associated telomere clustering and pairing precede meiotic chromosome synapsis in *Arabidopsis thaliana*. *Journal of Cell Science*, **114**, 4207–4217.
- Benoit, M., Simon, L., Desset, S., Duc, C., Cotterell, S., Poulet, A. *et al.* (2019) Replication-coupled histone H3.1 deposition determines nucleosome composition and heterochromatin dynamics during Arabidopsis seedling development. *The New Phytologist*, **221**, 385–398.
- Bouvier, D., Ferrand, J., Chevallier, O., Paulsen, M.T., Ljungman, M. & Polo, S.E. (2021) Dissecting regulatory pathways for transcription recovery following DNA damage reveals a non-canonical function of the histone chaperone HIRA. *Nature Communications*, **12**, 3835.
- Buschbeck, M. & Hake, S.B. (2017) Variants of core histones and their roles in cell fate decisions, development and cancer. *Nature Reviews. Molecular Cell Biology*, **18**, 299–314.
- Chandrasekhara, C., Mohannath, G., Blevins, T., Pontvianne, F. & Pikaard, C.S. (2016) Chromosome-specific NOR inactivation explains selective rRNA gene silencing and dosage control in Arabidopsis. *Genes & Development*, **30**, 177–190.
- Davarinejad, H., Huang, Y.C., Mermaz, B., LeBlanc, C., Poulet, A., Thomson, G. *et al.* (2022) The histone H3.1 variant regulates TONSOKU-mediated DNA repair during replication. *Science*, **375**, 1281–1286.
- de Lange, T. (2005) Shelterin: the protein complex that shapes and safeguards human telomeres. *Genes & Development*, **19**, 2100–2110.
- Dellaporta, S.L., Wood, J. & Hicks, J.B. (1983) A plant DNA miniprep: version II. *Plant Molecular Biology Reporter*, **1**, 19–21.
- Desset, S., Poulet, A. & Tatout, C. (2018) Quantitative 3D analysis of nuclear morphology and heterochromatin organization from whole-mount plant tissue using NucleusJ. *Methods in Molecular Biology*, **1675**, 615–632.
- Dewari, P.S. & Bhargava, P. (2014) Genome-wide mapping of yeast histone chaperone anti-silencing function 1 reveals its role in condensin binding with chromatin. *PLoS One*, **9**, e108652.
- Dreissig, S., Schiml, S., Schindele, P., Weiss, O., Rutten, T., Schubert, V. *et al.* (2017) Live-cell CRISPR imaging in plants reveals dynamic telomere

- movements. *The Plant Journal: For Cell and Molecular Biology*, **91**, 565–573.
- Dubos, T., Poulet, A., Gonthier-Gueret, C., Mougeot, G., Vanrobays, E., Li, Y. *et al.* (2020) Automated 3D bio-imaging analysis of nuclear organization by NucleusJ 2.0. *Nucleus*, **11**, 315–329.
- Duc, C., Benoit, M., Detourne, G., Simon, L., Poulet, A., Jung, M. *et al.* (2017) Arabidopsis ATRX modulates H3.3 occupancy and fine-tunes gene expression. *Plant Cell*, **29**, 1773–1793.
- Duc, C., Benoit, M., Le Goff, S., Simon, L., Poulet, A., Cotterell, S. *et al.* (2015) The histone chaperone complex HIR maintains nucleosome occupancy and counterbalances impaired histone deposition in CAF-1 complex mutants. *The Plant Journal*, **81**, 707–722.
- Dvorackova, M., Fojtova, M. & Fajkus, J. (2015) Chromatin dynamics of plant telomeres and ribosomal genes. *The Plant Journal: For Cell and Molecular Biology*, **83**, 18–37.
- Dvorackova, M., Rossignol, P., Shaw, P.J., Koroleva, O.A., Doonan, J.H. & Fajkus, J. (2010) AtTRB1, a telomeric DNA-binding protein from Arabidopsis, is concentrated in the nucleolus and shows highly dynamic association with chromatin. *The Plant Journal: For Cell and Molecular Biology*, **61**, 637–649.
- Edwards, K., Johnstone, C. & Thompson, C. (1991) A simple and rapid method for the preparation of plant genomic DNA for PCR analysis. *Nucleic Acids Research*, **19**, 1349.
- Eekhout, T., Dvorackova, M., Pedroza Garcia, J.A., Nespore Dadejova, M., Kalhorzadeh, P., Van den Daele, H. *et al.* (2021) G2/M-checkpoint activation in fasciata1 rescues an aberrant S-phase checkpoint but causes genome instability. *Plant Physiology*, **186**, 1893–1907.
- English, C.M., Adkins, M.W., Carson, J.J., Churchill, M.E. & Tyler, J.K. (2006) Structural basis for the histone chaperone activity of Asf1. *Cell*, **127**, 495–508.
- Exner, V., Taranto, P., Schonrock, N., Gruissem, W. & Hennig, L. (2006) Chromatin assembly factor CAF-1 is required for cellular differentiation during plant development. *Development*, **133**, 4163–4172.
- Fajkus, J., Fulneckova, J., Hulanova, M., Berkova, K., Riha, K. & Matyasek, R. (1998) Plant cells express telomerase activity upon transfer to callus culture, without extensively changing telomere lengths. *Molecular & General Genetics*, **260**, 470–474.
- Fajkus, J. & Trifonov, E.N. (2001) Columnar packing of telomeric nucleosomes. *Biochemical and Biophysical Research Communications*, **280**, 961–963.
- Feng, S., Ma, S., Li, K., Gao, S., Ning, S., Shang, J. *et al.* (2022) RIF1-ASF1-mediated high-order chromatin structure safeguards genome integrity. *Nature Communications*, **13**, 957.
- Fitzgerald, M.S., McKnight, T.D. & Shippen, D.E. (1996) Characterization and developmental patterns of telomerase expression in plants. *Proceedings of the National Academy of Sciences of the United States of America*, **93**, 14422–14427.
- Fitzgerald, M.S., Riha, K., Gao, F., Ren, S., McKnight, T.D. & Shippen, D.E. (1999) Disruption of the telomerase catalytic subunit gene from Arabidopsis inactivates telomerase and leads to a slow loss of telomeric DNA. *Proceedings of the National Academy of Sciences of the United States of America*, **96**, 14813–14818.
- Franz, P., de Jong, J.H., Lysak, M., Castiglione, M.R. & Schubert, I. (2002) Interphase chromosomes in are organized as well defined chromocenters from which euchromatin loops emanate. *Proceedings of the National Academy of Sciences of the United States of America*, **99**, 14584–14589.
- Fulneckova, J., Dokladal, L., Kolarova, K., Nespore Dadejova, M., Prochazkova, K., Gomelska, S. *et al.* (2021) Telomerase interaction partners-insight from plants. *International Journal of Molecular Sciences*, **23**, 368.
- Goldberg, A.D., Banaszynski, L.A., Noh, K.M., Lewis, P.W., Elsaesser, S.J., Stadler, S. *et al.* (2010) Distinct factors control histone variant H3.3 localization at specific genomic regions. *Cell*, **140**, 678–691.
- Greider, C.W. & Blackburn, E.H. (1985) Identification of a specific telomere terminal transferase activity in *Tetrahymena* extracts. *Cell*, **43**, 405–413.
- Greider, C.W. & Blackburn, E.H. (1996) Telomeres, telomerase and cancer. *Scientific American*, **274**, 92–97.
- Groth, A., Corpet, A., Cook, A.J., Roche, D., Bartek, J., Lukas, J. *et al.* (2007) Regulation of replication fork progression through histone supply and demand. *Science*, **318**, 1928–1931.
- Guthmann, M., Qian, C., Gialdini, I., Nakatani, T., Ettinger, A., Schauer, T. *et al.* (2023) A change in biophysical properties accompanies heterochromatin formation in mouse embryos. *Genes & Development*, **37**, 336–350.
- Hiraga, S., Botsios, S. & Donaldson, A.D. (2008) Histone H3 lysine 56 acetylation by Rtt109 is crucial for chromosome positioning. *The Journal of Cell Biology*, **183**, 641–651.
- Hoang, S.M., Kaminski, N., Bhargava, R., Barroso-Gonzalez, J., Lynskey, M.L., Garcia-Exposito, L. *et al.* (2020) Regulation of ALT-associated homology-directed repair by polyADP-ribosylation. *Nature Structural & Molecular Biology*, **27**, 1152–1164.
- Hofr, C., Sultesova, P., Zimmermann, M., Mozgova, I., Schrupfova, P.P., Wimmerova, M. *et al.* (2009) Single-Myb-histone proteins from *Arabidopsis thaliana*: a quantitative study of telomere-binding specificity and kinetics. *The Biochemical Journal*, **419**, 221–228.
- Huang, S., Zhou, H., Tarara, J. & Zhang, Z. (2007) A novel role for histone chaperones CAF-1 and Rtt106p in heterochromatin silencing. *The EMBO Journal*, **26**, 2274–2283.
- Jaske, K., Mokros, P., Mozgova, I., Fojtova, M. & Fajkus, J. (2013) A telomerase-independent component of telomere loss in chromatin assembly factor 1 mutants of *Arabidopsis thaliana*. *Chromosoma*, **122**, 285–293.
- Jiang, D. & Berger, F. (2017) DNA replication-coupled histone modification maintains polycomb gene silencing in plants. *Science*, **357**, 1146–1149.
- Jiang, W.Q., Nguyen, A., Cao, Y., Chang, A.C. & Reddel, R.R. (2011) HP1-mediated formation of alternative lengthening of telomeres-associated PML bodies requires HIRA but not ASF1a. *PLoS One*, **6**, e17036.
- Kannan, K., Nelson, A.D. & Shippen, D.E. (2008) Dyskerin is a component of the Arabidopsis telomerase RNP required for telomere maintenance. *Molecular and Cellular Biology*, **28**, 2332–2341.
- Kaufman, P.D., Kobayashi, R., Kessler, N. & Stillman, B. (1995) The p150 and p60 subunits of chromatin assembly factor I: a molecular link between newly synthesized histones and DNA replication. *Cell*, **81**, 1105–1114.
- Kaya, H., Shibahara, K.I., Taoka, K.I., Iwabuchi, M., Stillman, B. & Araki, T. (2001) FASCIATA genes for chromatin assembly factor-1 in Arabidopsis maintain the cellular organization of apical meristems. *Cell*, **104**, 131–142.
- Kerppola, T.K. (2008) Bimolecular fluorescence complementation (BiFC) analysis as a probe of protein interactions in living cells. *Annual Review of Biophysics*, **37**, 465–487.
- Kim, N.W., Piatyszek, M.A., Prowse, K.R., Harley, C.B., West, M.D., Ho, P.L. *et al.* (1994) Specific association of human telomerase activity with immortal cells and cancer. *Science*, **266**, 2011–2015.
- Kirik, A., Pecinka, A., Wendeler, E. & Reiss, B. (2006) The chromatin assembly factor subunit FASCIATA1 is involved in homologous recombination in plants. *Plant Cell*, **18**, 2431–2442.
- Klein, K.N., Zhao, P.A., Lyu, X., Sasaki, T., Bartlett, D.A., Singh, A.M. *et al.* (2021) Replication timing maintains the global epigenetic state in human cells. *Science*, **372**, 371–378.
- Klimovskaia, I.M., Young, C., Stromme, C.B., Menard, P., Jasencakova, Z., Mejlvang, J. *et al.* (2014) Tausled-like kinases phosphorylate Asf1 to promote histone supply during DNA replication. *Nature Communications*, **5**, 3394.
- Kolarova, K., Nespore Dadejova, M., Loja, T., Lochmanova, G., Sykorova, E. & Dvorackova, M. (2021) Disruption of NAP1 genes in *Arabidopsis thaliana* suppresses the fas1 mutant phenotype, enhances genome stability and changes chromatin compaction. *The Plant Journal*, **106**, 56–73.
- Lamour, V., Lecluse, Y., Desmaze, C., Spector, M., Bodescot, M., Aurias, A. *et al.* (1995) A human homolog of the *S. cerevisiae* HIR1 and HIR2 transcriptional repressors cloned from the DiGeorge syndrome critical region. *Human Molecular Genetics*, **4**, 791–799.
- Langmead, B., Trapnell, C., Pop, M. & Salzberg, S.L. (2009) Ultrafast and memory-efficient alignment of short DNA sequences to the human genome. *Genome Biology*, **10**, R25.
- Le Goff, S., Keceli, B.N., Jerabkova, H., Heckmann, S., Rutten, T., Cotterell, S. *et al.* (2020) The H3 histone chaperone NASP(SIM3) escorts CenH3 in Arabidopsis. *The Plant Journal: For Cell and Molecular Biology*, **101**, 71–86.
- Le, S., Davis, C., Konopka, J.B. & Sternglanz, R. (1997) Two new S-phase-specific genes from *Saccharomyces cerevisiae*. *Yeast*, **13**, 1029–1042.
- Lee, J.H., Lee, Y.S., Jeong, S.A., Khadka, P., Roth, J. & Chung, I.K. (2014) Catalytically active telomerase holoenzyme is assembled in the dense fibrillar component of the nucleolus during S phase. *Histochemistry and Cell Biology*, **141**, 137–152.



- Lermontova, I., Schubert, V., Bornke, F., Macas, J. & Schubert, I. (2007) Arabidopsis CBF5 interacts with the H/ACA snoRNP assembly factor NAF1. *Plant Molecular Biology*, **65**, 615–626.
- Lewis, P.W., Elsaesser, S.J., Noh, K.M., Stadler, S.C. & Allis, C.D. (2010) Daxx is an H3.3-specific histone chaperone and cooperates with ATRX in replication-independent chromatin assembly at telomeres. *Proceedings of the National Academy of Sciences of the United States of America*, **107**, 14075–14080.
- Li, F., Deng, Z., Zhang, L., Wu, C., Jin, Y., Hwang, I. et al. (2019) ATRX loss induces telomere dysfunction and necessitates induction of alternative lengthening of telomeres during human cell immortalization. *The EMBO Journal*, **38**, e96659.
- Lycka, M., Peska, V., Demko, M., Spyrglou, I., Kilar, A., Fajkus, J. et al. (2021) WALTER: an easy way to online evaluate telomere lengths from terminal restriction fragment analysis. *BMC Bioinformatics*, **22**, 145.
- McClintock, B. (1930) A cytological demonstration of the location of an interchange between two non-homologous chromosomes of *Zea mays*. *Proceedings of the National Academy of Sciences of the United States of America*, **16**, 791–796.
- Miller, K.E., Kim, Y., Huh, W.K. & Park, H.O. (2015) Bimolecular fluorescence complementation (BiFC) analysis: advances and recent applications for genome-wide interaction studies. *Journal of Molecular Biology*, **427**, 2039–2055.
- Min, Y., Frost, J.M. & Choi, Y. (2019) Nuclear chaperone ASF1 is required for gametogenesis in *Arabidopsis thaliana*. *Scientific Reports*, **9**(13), 959.
- Moshkin, Y.M., Armstrong, J.A., Maeda, R.K., Tamkun, J.W., Verrijzer, P., Kennison, J.A. et al. (2002) Histone chaperone ASF1 cooperates with the Brahma chromatin-remodelling machinery. *Genes & Development*, **16**, 2621–2626.
- Mougeot, G., Safarbaty, S., Alégot, H., Pouchin, P., Field, N., Almagro, S. et al. (2024) Biom3d, a modular framework to host and develop 3D segmentation methods. *bioRxiv*. Available from: <https://doi.org/10.1101/2024.07.25.60480>
- Mozgova, I., Mokros, P. & Fajkus, J. (2010) Dysfunction of chromatin assembly factor 1 induces shortening of telomeres and loss of 45S rDNA in *Arabidopsis thaliana*. *Plant Cell*, **22**, 2768–2780.
- Muchova, V., Amiard, S., Mozgova, I., Dvorackova, M., Gallego, M.E., White, C. et al. (2015) Homology-dependent repair is involved in 45S rDNA loss in plant CAF-1 mutants. *The Plant Journal*, **81**, 198–209.
- Munoz-Viana, R., Wildhaber, T., Trejo-Arellano, M.S., Mozgova, I. & Hennig, L. (2017) Arabidopsis chromatin assembly factor 1 is required for occupancy and position of a subset of nucleosomes. *The Plant Journal*, **92**, 363–374.
- Naish, M., Alonge, M., Wlodzimierz, P., Tock, A.J., Abramson, B.W., Schmucker, A. et al. (2021) The genetic and epigenetic landscape of the Arabidopsis centromeres. *Science*, **374**, eabi7489.
- Nersisyan, L. & Arakelyan, A. (2015) Computel: computation of mean telomere length from whole-genome next-generation sequencing data. *PLoS One*, **10**, e0125201.
- Nespor Dadejova, M., Franek, M. & Dvorackova, M. (2022) Laser microirradiation as a versatile system for probing protein recruitment and protein–protein interactions at DNA lesions in plants. *The New Phytologist*, **234**, 1891–1900.
- Nie, X., Wang, H., Li, J., Holec, S. & Berger, F. (2014) The HIRA complex that deposits the histone H3.3 is conserved in Arabidopsis and facilitates transcriptional dynamics. *Biology Open*, **3**, 794–802.
- Olovnikov, A.M. (1992) Aging is a result of a shortening of the “differotene” in the telomere due to end under-replication and under-repair of DNA. *Izvestiia Akademii nauk SSSR. Seriya Biologicheskaya*, 641–643.
- Ono, T., Kaya, H., Takeda, S., Abe, M., Ogawa, Y., Kato, M. et al. (2006) Chromatin assembly factor 1 ensures the stable maintenance of silent chromatin states in Arabidopsis. *Genes to Cells*, **11**, 153–162.
- O’Sullivan, R.J., Arnould, N., Lackner, D.H., Oganessian, L., Haggblom, C., Corpet, A. et al. (2014) Rapid induction of alternative lengthening of telomeres by depletion of the histone chaperone ASF1. *Nature Structural & Molecular Biology*, **21**, 167–174.
- Otero, S., Desvoyes, B., Peiro, R. & Gutierrez, C. (2016) Histone H3 dynamics reveal domains with distinct proliferation potential in the Arabidopsis root. *Plant Cell*, **28**, 1361–1371.
- Palm, W. & de Lange, T. (2008) How shelterin protects mammalian telomeres. *Annual Review of Genetics*, **42**, 301–334.
- Picart-Picoló, A., Grob, S., Picault, N., Franek, M., Llauro, C., Halter, T. et al. (2020) Large tandem duplications affect gene expression, 3D organization, and plant-pathogen response. *Genome Research*, **30**, 1583–1592.
- Pontvianne, F., Blevins, T., Chandrasekhara, C., Mozgova, I., Hassel, C., Pontes, O.M. et al. (2013) Subnuclear partitioning of rRNA genes between the nucleolus and nucleoplasm reflects alternative epiallelic states. *Genes & Development*, **27**, 1545–1550.
- Pontvianne, F., Carpentier, M.C., Durut, N., Pavlistova, V., Jaske, K., Schorova, S. et al. (2016) Identification of nucleolus-associated chromatin domains reveals a role for the nucleolus in 3D organization of the *A. thaliana* genome. *Cell Reports*, **16**, 1574–1587.
- Probst, A.V., Desvoyes, B. & Gutierrez, C. (2020) Similar yet critically different: the distribution, dynamics and function of histone variants. *Journal of Experimental Botany*, **71**, 5191–5204.
- Probst, A.V., Franz, P.F., Paszkowski, J. & Mittelsten Scheid, O. (2003) Two means of transcriptional reactivation within heterochromatin. *The Plant Journal: For Cell and Molecular Biology*, **33**, 743–749.
- Ray-Gallet, D., Quivy, J.P., Scamps, C., Martini, E.M., Lipinski, M. & Almouzni, G. (2002) HIRA is critical for a nucleosome assembly pathway independent of DNA synthesis. *Molecular Cell*, **9**, 1091–1100.
- Richards, E.J. & Ausubel, F.M. (1988) Isolation of a higher eukaryotic telomere from *Arabidopsis thaliana*. *Cell*, **53**, 127–136.
- Riha, K., McKnight, T.D., Griffing, L.R. & Shippen, D.E. (2001) Living with genome instability: plant responses to telomere dysfunction. *Science*, **291**, 1797–1800.
- Ruckova, E., Friml, J., Schrupfova, P.P. & Fajkus, J. (2008) Role of alternative telomere lengthening unmasked in telomerase knock-out mutant plants. *Plant Molecular Biology*, **66**, 637–646.
- Schorova, S., Fajkus, J., Zaveska Drabkova, L., Honys, D. & Schrupfova, P.P. (2019) The plant Pontin and Reptin homologues, RuvBL1 and RuvBL2a, colocalize with TERT and TRB proteins in vivo, and participate in telomerase biogenesis. *The Plant Journal: For Cell and Molecular Biology*, **98**, 195–212.
- Schrumpfova, P.P., Fojtova, M. & Fajkus, J. (2019) Telomeres in plants and humans: not so different, not so similar. *Cells*, **8**, 58.
- Schrumpfova, P.P., Vychodilova, I., Dvorackova, M., Majerska, J., Dokladal, L., Schorova, S. et al. (2014) Telomere repeat binding proteins are functional components of Arabidopsis telomeres and interact with telomerase. *The Plant Journal*, **77**, 770–781.
- Schrumpfova, P.P., Vychodilova, I., Hapala, J., Schorova, S., Dvoracek, V. & Fajkus, J. (2016) Telomere binding protein TRB1 is associated with promoters of translation machinery genes in vivo. *Plant Molecular Biology*, **90**, 189–206.
- Sharp, J.A., Fouts, E.T., Krawitz, D.C. & Kaufman, P.D. (2001) Yeast histone deposition protein Asf1p requires Hir proteins and PCNA for heterochromatic silencing. *Current Biology*, **11**, 463–473.
- Silverman, J., Takai, H., Buonomo, S.B.C., Eisenhaber, F. & de Lange, T. (2004) Human Rif1, ortholog of a yeast telomeric protein, is regulated by ATM and 53BP1 and functions in the S-phase checkpoint. *Genes & Development*, **18**, 2108–2119.
- Soman, A., Wong, S.Y., Korolev, N., Surya, W., Lattmann, S., Vogirala, V.K. et al. (2022) Columnar structure of human telomeric chromatin. *Nature*, **609**, 1048–1055.
- Song, J., Rutjens, B. & Dean, C. (2014) Detecting histone modifications in plants. *Methods in Molecular Biology*, **1112**, 165–175.
- Tagami, H., Ray-Gallet, D., Almouzni, G. & Nakatani, Y. (2004) Histone H3.1 and H3.3 complexes mediate nucleosome assembly pathways dependent or independent of DNA synthesis. *Cell*, **116**, 51–61.
- Tang, M., Chen, Z., Wang, C., Feng, X., Lee, N., Huang, M. et al. (2022) Histone chaperone ASF1 acts with RIF1 to promote DNA end joining in BRCA1-deficient cells. *The Journal of Biological Chemistry*, **298**(10), 979.
- Teano, G., Concia, L., Wolff, L., Carron, L., Biocanin, I., Adamusova, K. et al. (2023) Histone H1 protects telomeric repeats from H3K27me3 invasion in Arabidopsis. *Cell Reports*, **42**(112), 894.
- Timashev, L.A., Babcock, H., Zhuang, X. & de Lange, T. (2017) The DDR at telomeres lacking intact shelterin does not require substantial chromatin decompaction. *Genes & Development*, **31**, 578–589.
- Torne, J., Ray-Gallet, D., Boyarchuk, E., Garnier, M., Le Baccon, P., Coulon, A. et al. (2020) Two HIRA-dependent pathways mediate H3.3 de novo deposition and recycling during transcription. *Nature Structural & Molecular Biology*, **27**, 1057–1068.

- Tyler, J.K., Adams, C.R., Chen, S.R., Kobayashi, R., Kamakaka, R.T. & Kado-naga, J.T.** (1999) The RCAF complex mediates chromatin assembly during DNA replication and repair. *Nature*, **402**, 555–560.
- Typas, D.** (2023) Histone H3 and its chaperones. *Nature Structural & Molecular Biology*, **30**, 405.
- Vaquero-Sedas, M.I. & Vega-Palas, M.A.** (2013) Differential association of Arabidopsis telomeres and centromeres with histone H3 variants. *Scientific Reports*, **3**, 1202.
- Verreault, A., Kaufman, P.D., Kobayashi, R. & Stillman, B.** (1996) Nucleosome assembly by a complex of CAF-1 and acetylated histones H3/H4. *Cell*, **87**, 95–104.
- Vespa, L., Warrington, R.T., Mokros, P., Siroky, J. & Shippen, D.E.** (2007) ATM regulates the length of individual telomere tracts in Arabidopsis. *Proceedings of the National Academy of Sciences of the United States of America*, **104**, 18145–18150.
- Vrbsky, J., Akimcheva, S., Watson, J.M., Turner, T.L., Daxinger, L., Vyskot, B. et al.** (2010) siRNA-mediated methylation of Arabidopsis telomeres. *PLoS Genetics*, **6**, e1000986.
- Weinert, T.** (2005) Do telomeres ask checkpoint proteins: “gimme shelter-in”? *Developmental Cell*, **9**, 725–726.
- Wollmann, H., Holec, S., Alden, K., Clarke, N.D., Jacques, P.E. & Berger, F.** (2012) Dynamic deposition of histone variant H3.3 accompanies developmental remodeling of the Arabidopsis transcriptome. *PLoS Genetics*, **8**, e1002658.
- Wong, L.H., Ren, H., Williams, E., McGhie, J., Ahn, S., Sim, M. et al.** (2009) Histone H3.3 incorporation provides a unique and functionally essential telomeric chromatin in embryonic stem cells. *Genome Research*, **19**, 404–414.
- Wu, M.Y., Lin, C.Y., Tseng, H.Y., Hsu, F.M., Chen, P.Y. & Kao, C.F.** (2017) H2B ubiquitylation and the histone chaperone Asf1 cooperatively mediate the formation and maintenance of heterochromatin silencing. *Nucleic Acids Research*, **45**, 8225–8238.
- Wu, W., He, J.N., Lan, M., Zhang, P. & Chu, W.K.** (2021) Transcription-replication collisions and chromosome fragility. *Frontiers in Genetics*, **12** (804), 547.
- Yang, Y., Chen, Y., Zhang, C., Huang, H. & Weissman, S.M.** (2002) Nucleolar localization of hTERT protein is associated with telomerase function. *Experimental Cell Research*, **277**, 201–209.
- Zachova, D., Fojtova, M., Dvorackova, M., Mozgova, I., Lermontova, I., Peska, V. et al.** (2013) Structure–function relationships during transgenic telomerase expression in Arabidopsis. *Physiologia Plantarum*, **149**, 114–126.
- Zavodnik, M., Fajkus, P., Franek, M., Kopecky, D., Garcia, S., Dodsworth, S. et al.** (2023) Telomerase RNA gene paralogs in plants – the usual pathway to unusual telomeres. *The New Phytologist*, **239**, 2353–2366.
- Zhong, Z., Wang, Y., Wang, M., Yang, F., Thomas, Q.A., Xue, Y. et al.** (2022) Histone chaperone ASF1 mediates H3.3-H4 deposition in Arabidopsis. *Nature Communications*, **13**, 6970.
- Zhou, Y., Hartwig, B., James, G.V., Schneeberger, K. & Turck, F.** (2016) Complementary activities of TELOMERE REPEAT BINDING proteins and Polycomb group complexes in transcriptional regulation of target genes. *Plant Cell*, **28**, 87–101.
- Zhu, Y., Weng, M., Yang, Y., Zhang, C., Li, Z., Shen, W.H. et al.** (2011) Arabidopsis homologues of the histone chaperone ASF1 are crucial for chromatin replication and cell proliferation in plant development. *The Plant Journal*, **66**, 443–455.